ELSEVIER ELSEVIER

Contents lists available at ScienceDirect

Physica D

journal homepage: www.elsevier.com/locate/physd



Multi-d isothermal Euler flow: Existence of unbounded radial similarity solutions



Helge Kristian Jenssen a,*, Charis Tsikkou b

- ^a Department of Mathematics. Penn State University, University Park, State College, PA 16802, USA
- ^b Department of Mathematics, West Virginia University, Morgantown, WV 26506, USA

ARTICLE INFO

Article history: Received 15 April 2019 Received in revised form 5 March 2020 Accepted 4 April 2020 Available online 15 April 2020 Communicated by S. Wang

Keywords: Compressible Inviscid Unbounded solution Radial flow Similarity solution

ABSTRACT

We show that the multi-dimensional compressible Euler system for isothermal flow of an ideal, polytropic gas admits global-in-time, radially symmetric solutions with unbounded amplitudes due to wave focusing. The examples are similarity solutions and involve a converging wave focusing at the origin. At time of collapse, the density, but not the velocity, becomes unbounded, resulting in an expanding shock wave. The solutions are constructed as functions of radial distance to the origin r and time t. We verify that they provide genuine, weak solutions to the original, multi-d, isothermal Euler system.

While motivated by the well-known Guderley solutions to the full Euler system for an ideal gas, the solutions we consider are of a different type. In Guderley solutions an incoming shock propagates toward the origin by penetrating a stationary and "cold" gas at zero pressure (there is no counter pressure due to vanishing temperature upstream of the shock), accompanied by blowup of velocity and pressure, but not of density, at collapse. It is currently not known whether the full system admits unbounded solutions in the absence of zero-pressure regions. The present work shows that the simplified isothermal model does admit such behavior.

© 2020 Elsevier B.V. All rights reserved.

1. Introduction

We consider isothermal flow in n=2 or 3 space dimensions as described by the compressible Euler equations which express conservation of mass and linear momentum in the absence of viscous effects. The governing equations are:

$$\rho_t + \operatorname{div}_{\mathbf{x}}(\rho \mathbf{u}) = 0 \tag{1.1}$$

$$(\rho \mathbf{u})_t + \operatorname{div}_{\mathbf{x}}[\rho \mathbf{u} \otimes \mathbf{u}] + \operatorname{grad}_{\mathbf{x}} p = 0, \tag{1.2}$$

where the independent variables are time t and position $\mathbf{x} \in \mathbb{R}^n$, and the primary dependent variables are the density ρ and the fluid velocity \mathbf{u} . In isothermal flow the pressure p is a linear function of density:

$$p(\rho) = a^2 \rho \qquad (a > 0 \text{ constant}). \tag{1.3}$$

As a nonlinear system of conservation laws, shock waves will typically be present in the solution, and one must therefore consider weak solutions that allow for propagating discontinuities in the primary flow variables. In contrast to 1-d flow, where Glimm's theorem [1] provides global existence for Cauchy problems via

uniform variation estimates when the data have sufficiently small total variation, there is currently no corresponding existence result available for general multi-d systems. In particular, this is the case for the isothermal Euler model (1.1)–(1.2). (We comment further on existence results for multi-d Euler flows below.)

Multi-d flows of a compressible fluid can be exceedingly complicated, and it is reasonable to restrict attention to special types of solutions. One such class of solutions, of both theoretical and practical interest [2,3], is provided by *radial* flows. These are solutions in which the variables depend on position only through the distance $r = |\mathbf{x}|$ to the origin, and in addition the velocity field is purely radial: $\mathbf{u} = u_r^{\mathbf{x}}$. For such flows (1.1)–(1.2) reduce to

$$r^m \rho_t + (r^m \rho u)_r = 0 \tag{1.4}$$

$$r^{m}(\rho u)_{t} + (r^{m}(\rho u^{2} + p))_{r} = mr^{m-1}p, \tag{1.5}$$

where m = n - 1. For smooth flows (1.4)–(1.5) reduce further to

$$\rho_t + u\rho_r + \rho(u_r + \frac{mu}{r}) = 0 \tag{1.6}$$

$$u_t + uu_r + \frac{1}{2}p_r = 0. {(1.7)}$$

While this is formally a 1-d system, r being the only spatial variable, the multi-d character of the flow is reflected in the geometric source term $\frac{m\rho u}{r}$ in (1.6). The presence of this term explains why there is no straightforward generalization of Glimm's

^{*} Corresponding author. E-mail addresses: jenssen@math.psu.edu (H.K. Jenssen), tsikkou@math.wvu.edu (C. Tsikkou).

theorem to multi-d flows: no matter how small total variation the data have initially, waves moving toward the origin may gain in strength, precluding a priori estimates for the total variation at later times. In fact, the presence of the unbounded factor $\frac{1}{r}$ in the geometric source term indicates that the Euler model allows for *amplitude blowup* - as opposed to the well-known fact that gradient blowup (i.e., shock formation) can occur.

The present work is concerned with the construction of unbounded radial solutions to the isothermal Euler system. The blowup solutions we exhibit are "converging-diverging flows" in which a weak discontinuity (i.e., a discontinuity in the first derivatives of the flow variables) converges toward the origin, "collapses" there at some instant in time, and reflects off an expanding shock wave which interacts with the incoming flow. The blowup occurs at, and only at, the origin at the time of collapse. Thanks to invariance under translations in time, one is free to choose the time of collapse to be t=0, and this choice is built into the type of solutions we consider. The constructed solutions are globally defined on all of space–time.

In this work we restrict attention to *similarity solutions* of the form

$$\rho(t,r) = \operatorname{sgn}(t)|t|^{\beta} \Omega(\xi), \qquad u(t,r) = U(\xi), \tag{1.8}$$

where the similarity variable ξ is given by

$$\xi = \frac{\mathbf{r}}{t},\tag{1.9}$$

and with the similarity exponent β suitably chosen; see Theorem 1.1. It is well-known ([3–6]) that the Euler system admits similarity solutions, and (1.8)–(1.9) represent the specialization of these to the isothermal model.

Substitution of (1.8) into (1.6)–(1.7) yields an ODE system for Ω and U, the *similarity ODEs* (2.1)–(2.2), and our goal is to generate particular solutions of these which provides unbounded solutions of the original, isothermal Euler system (1.1)–(1.2). Specifically, the solutions we build suffer blowup of the density field, but not the velocity field, at the origin r=0 at time t=0.

To describe the relevance of our results we need to review in more detail what is known about radial solutions of the Euler system. In fact, the seminal work [4] by Guderley showed that already the physically more relevant full Euler system (i.e., including conservation of energy) for an ideal, polytropic gas, admits unbounded radial solutions of similarity type where a converging shock invades a quiescent state near the origin (i.e., the fluid is at rest and at constant density and pressure there), collapses at the origin with infinite speed, and generates an expanding shock wave. The work by Guderley has been revisited and extended by many researchers. E.g., Hunter [7] provided examples of similarity solutions describing the collapse of spherical cavities. The work of Lazarus [8] (building on earlier, joint work with Richtmyer, see the references in [8]) provided a detailed treatment of both the shock and the cavity problems, and also addressed the issue of stability of the blowup solutions. See also [9] which employs Guderley solutions as benchmarks for computational codes. We refer to the latter work for an extensive bibliography on Guderley solutions.

On the other hand, it is only recently that it has been demonstrated, in a mathematically rigorous manner, that the Guderley solutions provide weak solutions to the original, multi-d Euler system. As the flow involves unbounded quantities, this requires a careful argument, see [10]. (For what is required of a "weak solution", see Definition 5.1).

However, there is a further aspect of Guderley solutions that requires attention, and which directly motivates the present work. Namely, while these solutions unequivocally demonstrate the possibility of amplitude blowup in Euler flows, they are also at the borderline of the regime where one expects the Euler system to be physically accurate. More precisely, for the Guderley solutions to be exact weak solutions of the full Euler system, the sound speed must vanish identically within the quiescent region invaded by the converging shock. As remarked by Lazarus (p. 318 in [8]), this is the only unphysical aspect of the setup. For the ideal gas case under consideration, it follows that the incoming shock does not experience any upstream counter-pressure. The gas is at zero temperature there, and this is sometimes referred to as a "cold gas" assumption. We note that the lack of upstream counter-pressure is often formulated as a reasonable simplifying assumption, a "strong shock approximation". The present work concerns exact, weak solutions of the Euler system. We are not aware of rigorous results justifying the use of a strong shock approximation in this context.

It appears reasonable that this absence of counter-pressure in Guderley solutions facilitates unbounded growth of the shock speed, with concomitant increases in pressure and temperature in the immediate wake of the converging shock wave. It is therefore unclear whether this is the (or part of the) mechanism that drives the amplitude blowup in Guderley solutions for the full Euler system. The alternative is that the blowup is purely (or mainly) a geometric effect driven by wave focusing, much like what occurs for radial solutions of the linear, multi-d wave equation.

The main goal of the present work is to clarify the mechanism for amplitude blowup in radial Euler flows by showing that blowup can occur in radial isothermal flows (of similarity type) even in the presence of an everywhere strictly positive pressure field.

The isothermal solutions we construct are qualitatively different from the Guderley solutions described above. First, our flows are continuous up to collapse, involving a converging weak discontinuity (i.e., a jump in radial derivatives rather than a jump in primary flow variables), and second, the converging weak wave, as well as the reflected shock wave, propagate at finite, constant speed. The density remains strictly positive everywhere at all times. In fact, the density, and thus pressure, ahead of the converging weak discontinuity grows without bound as $t \uparrow 0$. This demonstrates that the geometric effect of wave focusing is sufficiently strong, on its own, to cause amplitude blowup — even in the presence of an increasing upstream pressure.

We expect that the same conclusion applies to the isentropic Euler model (i.e., (1.1)–(1.2) with $p(\rho)=a^2\rho^\gamma$ and $\gamma>1$), as well as to the full Euler model. However, it appears more challenging to build explicit examples of unbounded flows with strictly positive pressure fields for these models. As we shall see below, the isothermal model yields a particularly simple system of similarity ODEs where the equation for $U(\xi)$ decouples and can be analyzed in isolation.

It is a remarkable fact, first observed by Guderley [4] (according to [3], p. 420), that the similarity ODEs for even the full Euler model can be reduced to a single, first order ODE. However, this is an ODE for one dependent similarity variable (C, monitoring the sound speed) in terms of another dependent similarity variable (U, monitoring the fluid velocity). It does not involve the independent similarity variable $\xi = \frac{t}{r^{\lambda}}$ (where $\lambda \geq 1$) in this case. To generate solutions of convergent–divergent flows of physical interest in this context is more involved, and requires the resolution of a non-linear eigenvalue problem: for a given adiabatic constant γ , only particular similarity exponents λ are admissible. In contrast, for the isothermal model we consider in this work, we can analyze the similarity ODEs more directly. In particular, by directly constructing U and Ω as functions of ξ , we obtain a one-parameter family of blowup solutions.

The solutions we construct meet the following natural requirements:

- (A) the velocity vanishes at all times at the center of motion r = 0: $u(t, 0) \equiv 0$;
- (B) at any fixed location away from the origin the density and velocity approach finite limits as time tends to the time of collapse: for each fixed r > 0 the limits

$$\lim_{t \to 0} u(t, r) \quad \text{and} \quad \lim_{t \to 0} \rho(t, r) \tag{1.10}$$

exist as finite numbers u(0,r) and $\rho(0,r)$, respectively. Equivalently, $t\mapsto u(t,r)$ and $t\mapsto \rho(t,r)$ are continuous at t=0 for each fixed t>0.

Note that requirement (B) leaves open the possibility that $\rho(0,r)$ and/or u(0,r) may blow up as $r\downarrow 0$. In addition, as discussed above, a key requirement in this work is that the density, and hence the pressure, is strictly positive:

(C) the density is everywhere strictly positive: $\rho(t,r) > 0$ for all $(t,r) \in \mathbb{R} \times \mathbb{R}^+$.

With these preparations our main result can be stated as follows (see Theorem 6.4 for a more detailed statement):

Theorem 1.1. The isothermal Euler system (1.1)–(1.2) in space dimension n=2 or 3 admits radial similarity solutions that suffer amplitude blow up. More precisely, for each similarity exponent $\beta \in (1-n, \frac{1-n}{2})$, there are radial similarity solutions of the form

$$\rho(t, \mathbf{x}) = \operatorname{sgn}(t) |t|^{\beta} \Omega(\frac{|\mathbf{x}|}{t}), \qquad \mathbf{u}(t, \mathbf{x}) = U(\frac{|\mathbf{x}|}{t}),$$

in which a weak discontinuity converges toward the origin for t < 0 and generates unbounded density at the origin at time t = 0, resulting in a single, compressive and expanding circular (n = 2) or spherical (n = 3) shock wave for t > 0. The velocity remains globally bounded.

These solutions are weak solutions of the multi-d isothermal Euler system (1.1)–(1.2) (in the sense of Definition 5.1) and satisfy the requirements (A), (B), (C) above.

The proof of the theorem entails a study of the critical points of the similarity ODEs, as well as the Rankine–Hugoniot relations and admissibility conditions across the shock wave that emerges at the time of collapse. For the latter we use Lax' entropy condition, which in the present context amounts to compressibility: the density increases as the fluid crosses the shock surface (see [11], Section 8.3).

Having built the solutions $(\rho(t,\mathbf{x}),\mathbf{u}(t,\mathbf{x}))$, for all $(t,\mathbf{x}) \in \mathbb{R}_t \times \mathbb{R}_{\mathbf{x}}^n$, from the $(U(\xi),\Omega(\xi))$ -solutions of the similarity ODEs, we finally need to verify that they are indeed genuine weak solutions of the original, multi-d Euler system. For this we require that: (i) the conserved quantities map time continuously into $L^1_{loc}(\mathbb{R}_{\mathbf{x}}^n)$; (ii) all terms in the weak forms of the equations are locally integrable in space–time; and (iii) the weak forms of the equations are satisfied (see Definition 5.1).

Regarding the last requirement, we stress that what we verify is the weak form of the equations (1.1)–(1.2) themselves, i.e., without terms corresponding to initial data. Of course, given a weak solution (ρ, \mathbf{u}) defined on $\mathbb{R}_t \times \mathbb{R}_{\mathbf{x}}^n$, in the sense of Definition 5.1, one may restrict it to any time interval $[t_0, +\infty)$, $t_0 \in \mathbb{R}$, and ask if it also provides a weak solution to the Cauchy problem with initial data $(\rho(t_0, \cdot), \mathbf{u}(t_0, \cdot))$. It is straightforward to verify that this is automatically satisfied because of requirement (i): ρ and $\rho \mathbf{u}$ define strongly continuous maps from \mathbb{R}_t into $L^1_{loc}(\mathbb{R}^n_{\mathbf{x}})$. The continuity property (i) is explicitly verified in Lemma 6.1 for the similarity solutions under consideration in this work.

We do not address the general issue of uniqueness of flows in this work. This is a challenging question for hyperbolic conservation laws in general, and particularly in the setting of unbounded solutions. For the similarity solutions we consider below, the blowup in amplitude occurs only at time t=0, with a density of the form $\rho(0,\mathbf{x})=const.|\mathbf{x}|^{\beta}$, $(\beta<0)$ and a globally bounded velocity $\mathbf{u}(0,\mathbf{x})$. We stress that we do *not* know that the solution we construct for t>0 provides the unique, physically acceptable continuation of these initial data. All we can say is that, subject to requirements (A) and (B), it provides the unique continuation to t>0 within the class of similarity solutions (1.8) with a fixed similarity exponent β .

The solutions we build have the property that the flow is "strictly converging" at time of collapse: $\mathbf{u}(0,\mathbf{x}) \equiv U^*\frac{\mathbf{x}}{L}$, where U^* is a strictly negative number. Combined with the presence of an infinite density (and thus infinite pressure) at the center of motion at time t=0, it is reasonable to expect the emergence of an expanding shock wave. Our analysis demonstrates the existence of exact solutions of this type. However, we stress that other types of blowup solutions, of similarity type, are possible for other choices of the similarity exponent β . E.g., it is not necessary to have a weak discontinuity focusing on the origin — even a smooth, converging wave can produce blowup. Second, there are cases in which the converging flow blows up, but does not generate an outgoing shock wave and instead a smooth flow emerges for t>0. As a limiting case a weak, outgoing discontinuity can also be generated. See Remark 3.2.

We end this introduction with some remarks on what is known about existence of radial Euler flows with "general" initial data. First, there is currently no result for the full, multi-d Euler system, radial or not, that guarantees global-in-time existence. For radial *isentropic* flows (i.e., the pressure law is $p(\rho) =$ $a^2 \rho^{\gamma}$ with $\gamma > 1$) results by Chen-Perepelitsa [12] and Chen-Schrecker [13] provide existence of weak, finite energy solutions via the method of compensated compactness. In fact, the recent work [14] by Schrecker is the first to show that the solutions one obtains in this manner provide genuine weak solutions to the original, multi-d isentropic Euler system (1.1)-(1.2) on all of space (i.e., including the origin). These works provide weak solutions for general, finite energy data; however, they yield no information about the possibility/impossibility of amplitude blowup. There appears to be little hope of extending the compensated compactness approach to the radial full system, or even (for technical reasons related to a lack of entropies, [15]) to the radial, isothermal system we consider in the present paper.

As far as we know, the currently strongest, global existence result for the radial isothermal system applies to the case of *external* flows, i.e., for flows outside of a fixed ball, see [16–18]. The results of the present paper show that, in order to extend these results to solutions defined on all of space (i.e., including the origin), one must necessarily contend with unbounded solutions.

For results closer to the present work, which concerns concrete Euler flows in several space dimensions, we refer to Chapter 7 of Zheng's monograph [19] on multi-d Riemann problems, some of which generate purely radial flows. However, we stress that the radial flows we construct below are not solutions to multi-d Riemann problems. Specifically, the solutions we display are necessarily non-constant in the radial direction at all times.

The rest of the present paper is organized as follows. In Section 2 we record the similarity ODEs and provide the Rankine–Hugoniot relations and entropy conditions as expressed in terms of the similarity variables ξ , Ω , and U. Sections 3 and 4 provide the details of the construction of the radial velocity and the corresponding density for converging-diverging similarity flows of the type described above. In Section 5 we briefly recall the definition of weak solutions to the barotropic Euler system, including its formulation for the special case of radial solutions. In Section 6 we verify that the radial similarity flows we construct provide genuine weak solutions to the original, multi-d

isothermal Euler system. A detailed statement of the main result is given in Theorem 6.4. Finally, Section 7 collects a few additional observations about the flows constructed in this paper. Some proofs of technical results are collected in Appendix.

2. Similarity ODEs and jump relations

2.1. Similarity ODEs

Substituting the ansatz (1.8)–(1.9) into (1.6)–(1.7), with isothermal pressure $p(\rho)=a^2\rho$, yields the following system of similarity ODEs for $\Omega(\xi)$ and $U(\xi)$:

$$(U - \xi)\frac{\Omega'}{\Omega} + U' + \left(\beta + \frac{mU}{\xi}\right) = 0 \tag{2.1}$$

$$a^2 \frac{\Omega'}{\Omega} + (U - \xi)U' = 0, \tag{2.2}$$

where $'\equiv \frac{d}{d\xi}$. At this stage the parameter $\beta\in\mathbb{R}$ is free. A simplifying feature of the isothermal case is that the system of similarity ODEs provides a single, decoupled ODE for U: solving for $\frac{\Omega'}{\Omega}$ in (2.2) and substituting into (2.1) yield

$$U' = \frac{a^2}{(U - \xi)^2 - a^2} \left(\beta + \frac{mU}{\xi}\right). \tag{2.3}$$

Using this in (2.2) gives

$$\frac{\Omega'}{\Omega} = -\frac{U - \xi}{(U - \xi)^2 - a^2} \left(\beta + \frac{mU}{\xi}\right). \tag{2.4}$$

Before analyzing the similarity ODEs further we deduce the jump conditions for propagating discontinuities, expressed in similarity variables.

2.2. Rankine-Hugoniot and entropy conditions

Consider the radial isothermal Euler system (1.4)–(1.5), and assume that a discontinuity propagates along the path $r = \mathcal{R}(t)$. The Rankine–Hugoniot relations that express conservation of mass and momentum across the discontinuity are given by

$$\dot{\mathcal{R}}[\![\rho]\!] = [\![\rho u]\!] \tag{2.5}$$

$$\dot{\mathcal{R}}[\![\rho u]\!] = [\![\rho u^2 + p]\!],\tag{2.6}$$

where $\dot{} \equiv \frac{d}{dt}$. Here and below we use the convention that, for any quantity q = q(t, r), [q] denotes the jump in q as r decreases, i.e.

$$[q] := q_+ - q_- \equiv q(t, \mathcal{R}(t)+) - q(t, \mathcal{R}(t)-).$$

Next, as the local sound speed c in isothermal flow is constant, $c \equiv a$ (where a is as in (1.3)), the characteristic speeds are $u \pm a$. It follows that the Lax entropy condition (characteristics run into the shock as time increases, [11]) takes the following forms:

$$u_- > \dot{\mathcal{R}} + a > u_+$$
 for a 1-shock, (2.7)

and

$$u_{-} > \dot{\mathcal{R}} - a > u_{+}$$
 for a 2-shock. (2.8)

We next specialize to "similarity shocks" in radial isothermal flow: the shock is assumed to propagate along a path of the form $\xi \equiv \bar{\xi}$, i.e., $\mathcal{R}(t) = \bar{\xi}t$. Furthermore, it is assumed that the density and velocity on either side of the shock are of the form (1.8), with β taking the same value on both sides. Letting (U_+, Ω_+) and (U_-, Ω_-) denote the parts of the solution on the outside and inside of the shock, respectively ("outside" and "inside" refer to further away from and closer to r=0, respectively), the Rankine–Hugoniot relations (2.5)–(2.6) reduce to

$$\bar{\xi} \llbracket \Omega \rrbracket = \llbracket \Omega U \rrbracket$$

$$\bar{\xi} \llbracket \Omega U \rrbracket = \llbracket \Omega (U^2 + a^2) \rrbracket,$$

where $[\![\cdot]\!]$ now denotes jump across $\xi=\bar{\xi}.$ The entropy conditions (2.7)–(2.8) take the form

$$U_{-}(\bar{\xi}) > \bar{\xi} + a > U_{+}(\bar{\xi})$$
 for a 1-shock (2.9)

$$U_{-}(\bar{\xi}) > \bar{\xi} - a > U_{+}(\bar{\xi})$$
 for a 2-shock. (2.10)

Finally, setting $V_{\pm}:=U_{\pm}-\bar{\xi}$, where U_{\pm} denotes $U_{\pm}(\bar{\xi})$, the Rankine–Hugoniot conditions take the form $[\Omega V]=0$ and $[\Omega VU+a^2\Omega]=0$. It follows from these that $V_+V_-=a^2$, and that an equivalent form of the jump conditions is given by

$$U_{+} = \bar{\xi} + \frac{a^2}{U_{-} - \bar{\xi}}$$
 and $\Omega_{+} = \frac{(U_{-} - \bar{\xi})^2}{a^2} \Omega_{-}.$ (2.11)

Alternatively, solving for V_{-} and Ω_{-} , we have

$$U_{-} = \bar{\xi} + \frac{a^2}{U_{+} - \bar{\xi}}$$
 and $\Omega_{-} = \frac{(U_{+} - \bar{\xi})^2}{a^2} \Omega_{+}.$ (2.12)

3. Construction of the velocity field

To construct relevant examples of converging-diverging isothermal similarity flows, we start with the ODE (2.3) for the velocity $U(\xi)$, which we now write as

$$U'(\xi) = \frac{F(\xi, U)}{G(\xi, U)},\tag{3.1}$$

where

$$F(\xi, U) = a^2(\beta \xi + mU)$$
 and $G(\xi, U) = \xi((U - \xi)^2 - a^2)$.

We shall make use of three solutions of (3.1), which together define, via $(1.8)_2$, the velocity field u(t,r) for all $(t,r) \in \mathbb{R} \times (0,\infty)$. The three U-solutions, denoted U_k , \hat{U} , \tilde{U} , will be defined on certain intervals, $(-\infty,\xi_w]$, $[\xi_w,\xi_s)$, and $[\xi_s,+\infty)$, respectively. The values $\xi_w<0$ and $\xi_s>0$ will give the paths $\{r=\xi_wt,\ t<0\}$ and $\{r=\xi_st,\ t>0\}$ of the converging weak discontinuity and expanding shock in our solutions, respectively; they are determined as part of the construction below. Then:

• U_{ν} will determine u within the sector

$$S_k := \{(r, t) \mid -\infty < \frac{r}{t} < \xi_w\},$$
 (3.2)

 \bullet \tilde{U} will determine u within the sector

$$\tilde{S} := \{ (r, t) \mid \xi_{s} < \frac{r}{t} < +\infty \}, \text{ while}$$
(3.3)

• \hat{U} will determine u within the two sectors

$$\hat{S}_{-} := \{(r, t) \mid \xi_{W} < \frac{r}{t} < 0\} \text{ and } \hat{S}_{+} := \{(r, t) \mid 0 < \frac{r}{t} < \xi_{S}\}.$$
(3.4)

Remark 3.1. As the following analysis shows, once we decide to search for similarity solution in which a weak discontinuity approaches the origin for t < 0, followed by an expanding shock for t > 0, then the requirements (A) and (B) in Section 1 will put certain constraints on the similarity exponent β . The constraints $1 - n < \beta < \frac{1-n}{2}$ in Theorem 1.1 provide *sufficient* conditions for generating the sought-for solution structure.

To determine the U_k , \hat{U} , \tilde{U} solutions we start by analyzing the critical points of (3.1).

3.1. Critical points

The number and locations of the critical points of (3.1) (i.e., the points where F and G vanish simultaneously) vary with the values of β and m = n - 1. It turns out that for our purpose of generating

particular blowup solutions, it suffices to restrict attention to the following cases:

$$-m < \beta < 0$$
 and $m = 1$ or $m = 2$, (3.5)

and we do so from here on; a further restriction will be added later (see Lemma 3.4). It is convenient to introduce the ratio

$$\mu := \frac{\beta}{m}$$
, so that $\mu \in (-1, 0)$,

and the straight lines in the (ξ, U) -plane given by

$$l_{+} := \{(\xi, U) \mid U = \xi \pm a\}$$
 and $\omega := \{(\xi, U) \mid U = -\mu \xi\}.$

The critical points of (3.1) are the points of intersection of ω (where F vanishes) with the U-axis and the lines l_{\pm} (where G vanishes). For the case (3.5) under consideration it follows (see Fig. 1) that (3.1) has three critical points: the origin (0, 0) and the points $\pm P_{\rm W} := (\pm \xi_{\rm W}, \pm U_{\rm W})$, where

$$\xi_{\rm W} := -\frac{a}{1+\mu} < 0, \qquad U_{\rm W} := \frac{a\mu}{1+\mu} < 0.$$
 (3.6)

(The subscript "w" is for "weak" as a weak discontinuity will propagate along $r = \xi_w t$, for t < 0, in the solutions to be constructed.) We also note that solutions of (3.1) are symmetric about the origin in the (ξ, U) -plane: if $\xi \mapsto U(\xi)$ is a solution, then so is $\xi \mapsto -U(-\xi)$.

3.2. Solution behavior near critical points

For each critical point $(\bar{\xi}, \bar{U})$ of (3.1) we linearize the ODE about it: the result is the ODE

$$U'(\xi) = \frac{C(\xi - \bar{\xi}) + D(U - \bar{U})}{A(\xi - \bar{\xi}) + B(U - \bar{U})}$$
(3.7)

where the coefficients are given by

$$A = (\bar{U} - \bar{\xi})^2 - 2\bar{\xi}(\bar{U} - \bar{\xi}) - a^2, \qquad B = 2\bar{\xi}(\bar{U} - \bar{\xi}),$$

$$C = a^2\beta, \qquad D = a^2m.$$

The type of the critical point $(\bar{\xi},\bar{U})$ is thus determined by the eigen-structure of the matrix

$$M \equiv M(\bar{\xi}, \bar{U}) = \left[\begin{array}{cc} A & B \\ C & D \end{array} \right].$$

This is detailed in the following two lemmas for $(\bar{\xi}, \bar{U}) = (0, 0)$ and $(\bar{\xi}, \bar{U}) = P_{\rm w}$, respectively. By symmetry of solutions of (3.1) about the origin, the type of the critical point $-P_{\rm w}$ is the same as that of $P_{\rm w}$. As we shall see, the three critical points of (3.1) under consideration are all hyperbolic (i.e., the real part of the eigenvalues of M are non-zero). It follows that the local behavior of solutions to (3.1) near the critical points agrees with that of its linearization.

Lemma 3.1. Consider the ODE (3.1) and assume (3.5) is satisfied. Then the critical point $(\bar{\xi}, \bar{U}) = (0, 0)$ is a saddle point for the linearized equation (3.7); the eigen-directions in the (ξ, U) -plane corresponding to the negative and positive eigenvalues of M(0, 0) are along $(n, -\beta)$ and (0, 1), respectively.

Proof. Evaluating the matrix M at $(\bar{\xi}, \bar{U}) = (0, 0)$ gives

$$M = M(0,0) = \begin{bmatrix} -a^2 & 0 \\ a^2\beta & a^2m \end{bmatrix},$$

which has eigenvalues $-a^2 < 0$ and $a^2m > 0$, with corresponding right eigenvectors $[n, -\beta]^T$ and $[0, 1]^T$, respectively. The result follows. \Box

Lemma 3.2. Consider the ODE (3.1) and assume (3.5) is satisfied. Then the critical point $(\bar{\xi}, \bar{U}) = (\xi_w, U_w)$ is a node for the linearized equation (3.7). More precisely, the eigenvalues of $M(\xi_w, U_w)$ are given by

$$\lambda_{\pm} = \frac{a^2}{2} \left[m + \frac{2}{1+\mu} \pm \sqrt{(m + \frac{2}{1+\mu})^2 - 8m} \right].$$
 (3.8)

Under assumption (3.5), λ_{\pm} are real and satisfy $0 < \lambda_{-} < \lambda_{+}$. The eigen-directions in the (ξ, U) -plane corresponding to λ_{-} and λ_{+} are along

$$(a^2m - \lambda_-, -a^2\beta)$$
 and $(a^2m - \lambda_+, -a^2\beta)$, (3.9) respectively.

Proof. Evaluating the matrix M at $(\bar{\xi}, \bar{U}) = (\xi_w, U_w)$ gives

$$M = M(\xi_{\rm w}, U_{\rm w}) = \begin{bmatrix} \frac{2a^2}{1+\mu} & -\frac{2a^2}{1+\mu} \\ a^2\beta & a^2m \end{bmatrix},$$

whose eigenvalues are given by (3.8). Assumption (3.5) yields $\frac{1}{1+\mu} > 1$, and since $m^2 + 4m + 4 \ge 8m$ and m > 0, we obtain that $(m + \frac{2}{1+\mu})^2 = m^2 + \frac{4m}{1+\mu} + \frac{4}{(1+\mu)^2} > 8m$. It follows that the radicand in (3.8) is strictly positive and that $0 < \lambda_- < \lambda_+$. A direct calculation yields the eigen-directions recorded in (3.9). \square

We record the following inequalities which will be used to deduce information about the structure of solutions to (3.1).

Lemma 3.3. With the notation as in Lemma 3.2, and under assumption (3.5), the following inequalities hold:

$$-\frac{a^{2}\beta}{a^{2}m-\lambda_{+}}<0<-\mu<-\frac{a^{2}\beta}{a^{2}m-\lambda_{-}}<1. \tag{3.10}$$

Proof. See Appendix. □

We proceed to employ the preceding lemmas to identify the solutions U_k , \hat{U} , and \tilde{U} of (3.1) that will be used to build the velocity field u(t, r).

3.3. Step 1: Solving (3.1) on
$$(-\infty, \xi_w]$$

It follows from Lemmas 3.2 and 3.3 that there is a unique solution of (3.1) that approaches $P_{\rm w}$ from the left (i.e., as $\xi \uparrow \xi_{\rm w}$) with negative slope $-\frac{a^2\beta}{a^2m-\lambda_+}$. We denote this particular solution curve by $U_{\rm k}(\xi)$; "k" is for "kink" as it provides the velocity of our solution on one side of the kink (weak discontinuity) that converges toward the origin. We shall argue that the solution $U_{\rm k}(\xi)$ is defined for all $\xi \leq \xi_{\rm w}$, and furthermore that, under certain conditions, it tends to a finite and strictly negative value U^* as $\xi \downarrow -\infty$. See Fig. 1.

To analyze U_k in more detail we first introduce the region

$$\mathcal{U} := \{ (\xi, U) : \xi < \xi_{W}, U > -\mu \xi \}.$$

We note that \mathcal{U} has $P_{\rm w}$ as corner point, and that $F|_{\mathcal{U}}>0$ and $G|_{\mathcal{U}}<0$. Since $U_{\rm k}$ approaches $P_{\rm w}$ from within \mathcal{U} , and since $F(\xi,U)/G(\xi,U)$ is a bounded function on $\mathcal{U}\smallsetminus B_{\varepsilon}$, for any ball B_{ε} centered at $P_{\rm w}$, it follows that the solution $U_{\rm k}(\xi)$ is defined for all $\xi<\xi_{\rm w}$ and that $U_{\rm k}'(\xi)<0$ for all such ξ . In particular, $U_{\rm k}(\xi)$ remains inside \mathcal{U} and satisfies

$$U_{\mathbf{k}}(\xi) > U_{\mathbf{w}} \quad \text{for } \xi < \xi_{\mathbf{w}}.$$
 (3.11)

We next analyze how $U_k(\xi)$ behaves for large, negative ξ -values. We shall see that it will tend to a finite limit at $\xi=-\infty$. Note that, since $\xi=\frac{r}{t}\to -\infty$ for r>0 fixed as $t\uparrow 0$, this finiteness of $U^*=U_k(-\infty)$ is required by the first part of requirement (B) in Section 1.

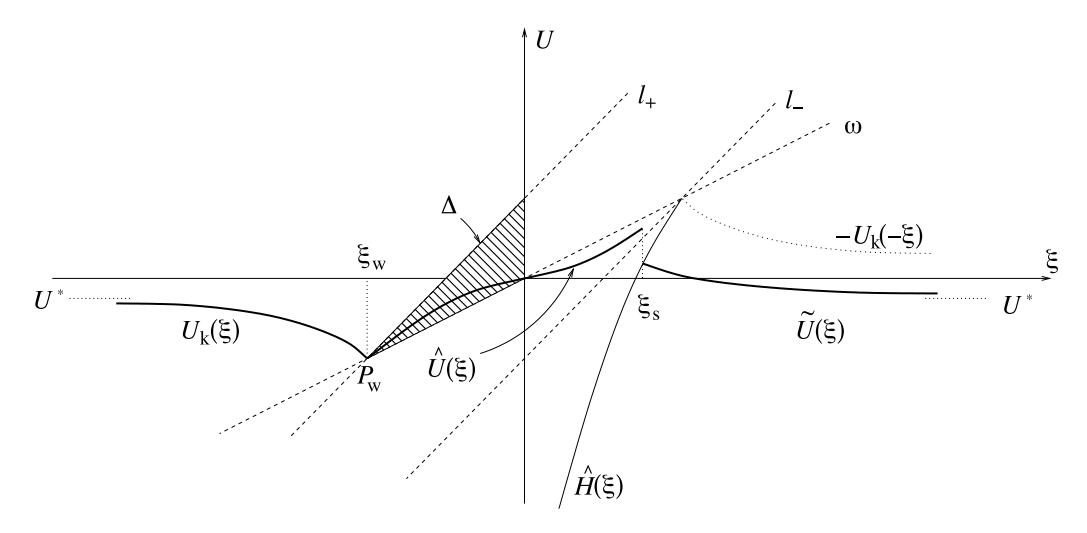


Fig. 1. Complete $U(\xi)$ -profile (schematic).

However, for the subsequent analysis we shall also need that $U^* < 0$. (Specifically, this is required to build a solution in which an expanding shock is present for t > 0; see Remark 3.2.) We proceed to show that there are solutions satisfying this constraint (as well as the constraints in (3.5)). We start by observing that for $(\xi, U) \in \mathcal{U}$ we have $U - \xi - a > U + \mu \xi > 0$, so that

$$\frac{U+\mu\xi}{U-\xi-a}<1\qquad\text{within }\mathcal{U}.$$

The solution U_k therefore satisfies

$$U_{\mathbf{k}}'(\xi) = \frac{a^2 m(U_{\mathbf{k}}(\xi) + \mu \xi)}{\xi(U_{\mathbf{k}}(\xi) - \xi - a)(U_{\mathbf{k}}(\xi) - \xi + a)} > \frac{a^2 m}{\xi(U_{\mathbf{k}}(\xi) - \xi + a)}.$$

Since $U_k(\xi)$ also satisfies (3.11), we obtain

$$U_{\mathsf{k}}'(\xi) > \frac{a^2m}{\xi(U_{\mathsf{k}}(\xi) - \xi + a)} > \frac{a^2m}{\xi(U_{\mathsf{w}} - \xi + a)} \qquad \text{for all } \xi < \xi_{\mathsf{w}}.$$

Integrating from $\xi < \xi_w$ to ξ_w gives

$$U_{k}(\xi) < U_{w} + a^{2}m \int_{\xi}^{\xi_{w}} \frac{d\xi}{\xi(\xi - (a + U_{w}))}, \qquad \xi < \xi_{w}.$$

Since $U_k(\xi)$ increases as ξ decreases, and since the last integral converges as $\xi \downarrow -\infty$, we conclude that the limit

 $U^* := U_k(-\infty)$ exists as a finite number.

Sending $\xi \downarrow -\infty$ and evaluating the resulting integral, we obtain that

$$U^* < U_{\rm w} + a^2 m \int_{-\infty}^{\xi_{\rm w}} \frac{d\xi}{\xi(\xi - (a + U_{\rm w}))}$$

$$= a \left[\frac{\mu}{1 + \mu} + \frac{m(1 + \mu)}{(1 + 2\mu)} \log(2(1 + \mu)) \right]. \tag{3.12}$$

Lemma 3.4. The function

$$L_m(\mu) := \frac{\mu}{1+\mu} + \frac{m(1+\mu)}{(1+2\mu)} \log(2(1+\mu))$$

appearing in (3.12) satisfies $L_m(\mu) < 0$ for $\mu \in (-1, -\frac{1}{2})$ for each of m = 1 and m = 2.

Proof. See Appendix. □

We note that, in terms of n=m+1 and β , the requirement $\mu=\frac{\beta}{m}\in(-1,-\frac{1}{2})$ takes the form (cf. Theorem 1.1)

$$\beta \in (1 - n, \frac{1 - n}{2}),\tag{3.13}$$

and this is assumed from now on.

Lemma 3.5. Under the requirement (3.13), we have that the kinksolution $U_k(\xi)$ tends to a finite and strictly negative limit as $\xi \downarrow -\infty$:

$$U^* := U_k(-\infty) < 0.$$

Proof. This is a direct consequence of Lemma 3.4 and (3.12). \Box

3.4. Step 2: Solving (3.1) on
$$\xi \in [\xi_w, \xi_s]$$

It follows from Lemmas 3.2 and 3.3 that among the solutions of (3.1) that emanate from $P_{\rm w}$ as ξ increases from $\xi_{\rm w}$, all but one starts out from $P_{\rm w}$ with positive slope $-\frac{a^2\beta}{a^2m-\lambda_-}$. (The exception is the solution which starts out with the slope $U'_{\rm k}(\xi_{\rm w})$; it will play no role in our analysis.) The two last inequalities in Lemma 3.3 further show that they all initially (i.e., for $\xi \gtrsim \xi_{\rm w}$) enter the triangle

$$\Delta := \{(\xi, U) \mid \xi_{W} < \xi < 0, -\mu \xi < U < \xi + a\},\$$

i.e., the triangle bounded by the U-axis, and the lines ω and l_+ (the shaded region in Fig. 1). An inspection of the phase portrait of (3.1) within Δ shows that, as ξ increases from $\xi_{\rm W}$ toward 0, each of these solutions, with one exception, meets the boundary of Δ either with infinite slope along the upper edge along l_+ , or with slope 0 at along the lower edge along ω . The sole exception is the unique solution (separatrix) which starts at $P_{\rm W}$, remains inside Δ , and (according to Lemma 3.1) reaches (0,0) with positive slope $-\frac{\beta}{n}$. By exploiting the symmetry of solutions to (3.1) about the origin in the (ξ, U) -plane, this solution may be continued (smoothly) up to $\xi = -\xi_{\rm W} > 0$. However, in our subsequent construction we shall only use $\hat{U}(\xi)$ for $\xi \in (\xi_{\rm W}, \xi_{\rm S})$, where $\xi_{\rm S} \in (0, -\xi_{\rm W})$, yet to be determined, gives the path $r = \xi_{\rm S}t$ of the reflected shock wave; see Fig. 1. We denote the solution under consideration, viewed as a function defined for $\xi \in (\xi_{\rm W}, \xi_{\rm S})$, by $\hat{I}(\xi)$

We stress that the use of \hat{U} is dictated, via $(1.8)_2$, by the physical requirement (A) above: we must have $\hat{U}(0) = 0$ in order that the fluid at the center of motion be at rest. The value of ξ_s will be determined once we have identified the relevant solution $\tilde{U}(\xi)$ of (3.1) to be used for large positive values of ξ .

3.5. Step 3: Solving (3.1) on $\xi \in [\xi_{s}, +\infty)$

Recall that U_k and \tilde{U} are to determine the velocity field u(t,r)within the two adjacent sectors S_k and \tilde{S} , respectively, which are separated by the positive r-axis; see (3.2) and (3.3). According to requirement (B) in Section 1, u(t, r) should be continuous across the positive r-axis. Since approaching a point (r, 0) on the positive *r*-axis from below or above, corresponds to ξ approaching $-\infty$ or $+\infty$, respectively, and $u(t,r)=U(\xi)$, we must have $\tilde{U}(+\infty)=$ $U_k(-\infty) = U^*$. Therefore, the relevant solution \tilde{U} of (3.1), to be used for $\xi \in (\xi_s, +\infty)$, is determined by the requirement that

$$\tilde{U}(+\infty) = U^*. \tag{3.14}$$

Next, as we integrate (3.1) along decreasing ξ -values from $\xi = +\infty$ in the (ξ, U) -plane, the graph of the solution $\tilde{U}(\xi)$ will remain below the graph of the function $-U_k(-\xi)$. This follows since the latter is a solution of (3.1) (recall that solutions of (3.1)lie symmetrically about the origin), which starts out from $\xi =$ $+\infty$ with the value $-U^* > 0 > U^*$.

Since the graph of $-U_k(-\xi)$ passes through $-P_w \in l_-$, it follows that the solution $\tilde{U}(\xi)$ intersects the straight line l_{-} (with slope $-\infty$) at some ξ -value ξ^* with $0<\xi^*<-\xi_{\rm w}$; see Fig. 1. The entire graph of $\tilde{U}(\xi)$, for $\xi^* < \xi < +\infty$, is therefore located below the line l_{-} and in the right half of the (ξ, U) -plane. (In particular, it follows from (3.1) that $\tilde{U}'(\xi) < 0$ for all $\xi \in (\xi^*, +\infty)$.)

Next, to determine the shock location ξ_s we argue as follows. Returning to the solution $\hat{U}(\xi)$ determined earlier, but now considered only for arguments $\xi \in (0, -\xi_{\rm W}]$, we let $\hat{\mathcal{H}}$ denote its associated "Hugoniot locus". That is, $\hat{\mathcal{H}}$ is the set of points $(\xi, \hat{H}(\xi))$ in the (ξ, U) -plane that connect to a point on the solution curve $(\xi, \hat{U}(\xi))$ through a jump discontinuity with $U_{-} = \hat{U}(\xi)$ and $U_+ = \hat{H}(\xi)$ (recall the notation from Section 2.2). According to $(2.11)_1$, $\hat{\mathcal{H}}$ is the graph of the function

$$\hat{H}(\xi) := \xi + \frac{a^2}{\hat{U}(\xi) - \xi} \qquad \text{for } 0 < \xi < -\xi_{\text{w}}.$$

The following lemma follows from the properties of the solution $\hat{U}(\xi)$. (See Fig. 1 where the graph of \hat{H} is drawn as a thin, solid curve.)

Lemma 3.6. The function $\hat{H}(\xi)$ has the following properties:

- (i) $\hat{H}(\xi) < \xi a$ for $0 < \xi < -\xi_w$, (ii) $\lim_{\xi \downarrow 0} \hat{H}(\xi) = -\infty$, and
- (iii) $\hat{H}(-\xi_{\rm w}) = -U_{\rm w}$.

Proof. See Appendix.

We conclude from Lemma 3.6 that the graphs of the functions $\hat{H}(\xi)$ and $\tilde{U}(\xi)$ intersect for at least one ξ -value between 0 and $-\xi_{w}$.

Remark 3.2. It is for this part of the argument that we require $U^* = U_k(-\infty) < 0$: only in this case does the solution contain an expanding shock for t > 0. If instead $U^* > 0$, then the solution $U(\xi)$ (obtained by integrating (3.1) in from $\xi = +\infty$ with $U(+\infty) = U^*$) will connect smoothly with $U(\xi)$ at $\xi = -\xi_w > 0$; no shock appears in the resulting flow. The limiting case where $U^* = 0$ is special: $U(\xi)$ then coincides with the solution $-U_k(-\xi)$ for $\xi \in (-\xi_w, +\infty)$; no shock appears, but there is a weak discontinuity expanding along $r = -\xi_w t$ for t > 0.

Also, in our setup above, we have chosen to use the "kinksolution" $U_k(\xi)$ for $\xi < \xi_w$. We could just as well have used one of the (infinitely many) solutions to (3.1) that connects smoothly with $\hat{U}(\xi)$ at $\xi = \xi_w$. The resulting flow would exhibit a smooth, converging wave. We omit the detailed arguments for these properties.

(As in Fig. 1, numerical calculations indicate that $\hat{H}(\xi)$ is strictly increasing on $(0, -\xi_w)$; if so, the point of intersection is uniquely determined. However, we have not been able to provide an analytic proof that $\hat{H}'(\xi) > 0$. On the other hand, should there be multiple ξ -values where $\hat{H}(\xi)$ and $\tilde{U}(\xi)$ agree, any one of these will work in the following argument.) Let $\xi_s \in (0, -\xi_w)$ be any value for which $\hat{H}(\xi_s) = \tilde{U}(\xi_s)$. We use this ξ_s -value to define the expanding shock path $r = \xi_s t$ in the (r, t)-plane across which the *U*-solution jumps from the value $U_{-}(\xi_s) := \hat{U}(\xi_s)$ on the inside, to the value $U_+(\xi_s) := \tilde{U}(\xi_s)$ on the outside. This defines a propagating jump discontinuity which, by construction, satisfies the first of the Rankine-Hugoniot jump conditions in (2.11). (The second one will be addressed in the construction of the similarity variable $\Omega(\xi)$.)

Finally, it follows from the construction of the function \hat{U} that $\xi > \hat{U}(\xi) > \xi - a$ for $\xi \in (0, -\xi_w)$. In particular,

$$\xi_{\rm S} > U_{-}(\xi_{\rm S}) \equiv \hat{U}(\xi_{\rm S}) > \xi_{\rm S} - a > \hat{H}(\xi_{\rm S}) = \tilde{U}(\xi_{\rm S}) \equiv U_{+}(\xi_{\rm S}),$$
 (3.15)

where the second inequality follows from part (i) of Lemma 3.6. We conclude from (2.10) that the jump discontinuity constructed above satisfies the entropy condition for a 2-shock.

We summarize the properties of the constructed velocity field in the following proposition.

Proposition 3.7. For space dimensions n = 2 or n = 3, let $\beta \in (1-n, \frac{1-n}{2})$. Consider the solutions U_k , \hat{U} , \tilde{U} of the similarity ODE (3.1) constructed above, and let the values $\xi_w < 0$ and $\xi_s > 0$ be determined as in (3.6) and in the present section, respectively. Then the functions u(t, r) and $U(\xi)$ defined by

$$u(t,r) = U(\frac{r}{t}) := \begin{cases} U_{\mathbf{k}}(\frac{r}{t}) & -\infty < \frac{r}{t} \le \xi_{\mathbf{w}} \\ \hat{U}(\frac{r}{t}) & \xi_{\mathbf{w}} \le \frac{r}{t} < \xi_{\mathbf{s}} \\ \tilde{U}(\frac{r}{t}) & \xi_{\mathbf{s}} < \frac{r}{t} < \infty, \end{cases}$$
(3.16)

together with

$$u(0,r) := U^* = U_k(-\infty),$$
 (3.17)

provides a globally bounded velocity field in which a weak discontinuity converges toward the origin along $r = \xi_w t$ for t < 0, and a diverging jump discontinuity, satisfying the Rankine-Hugoniot jump condition in $(2.11)_1$ and the entropy condition (2.10) for a 2-shock, diverges from the origin along $r = \xi_s t$ for t > 0. Finally,

$$u(t,0) \equiv 0$$
 and $u(0,r) \equiv U^*$, (3.18)

and u(t,r) satisfies the physical requirements (A) and (B) in Section 1.

Remark 3.3. With the setup of Proposition 3.7 the function $U(\xi)$ is strictly decreasing on (ξ_s, ∞) and tends to $U^* < 0$ as $\xi \rightarrow$ ∞ . Numerical calculations show that there are cases for which $U(\xi_s) > 0$. It follows that there exists a ξ -value for which $U(\xi)$ vanishes. This shows that stagnation (vanishing flow velocity) may occur upstream of the expanding shock. On the other hand, under the assumptions in Proposition 3.7, no stagnation occurs in the solution for t < 0.

4. Construction of the density field

Having constructed the velocity field u as described in Proposition 3.7, we proceed to build a corresponding density field $\rho(t,r)$ of the similarity type

$$\rho(t,r) = \operatorname{sgn}(t)|t|^{\beta} \Omega(\xi), \qquad \qquad \xi = \frac{r}{t}, \tag{4.1}$$

where Ω solves the second similarity ODE (2.2), repeated here for convenience in the form:

$$\Omega'(\xi) = V(\xi)\Omega(\xi),\tag{4.2}$$

where, according to (3.1),

$$V(\xi) := -\frac{1}{a^2} (U(\xi) - \xi) U'(\xi)$$

$$= -\frac{(U(\xi) - \xi)(\beta \xi + mU(\xi))}{\xi((U(\xi) - \xi)^2 - a^2)}, \quad \xi \in \mathbb{R}.$$
(4.3)

Here, $U(\xi)$ is given by Proposition 3.7 and consists of the three parts U_k , \hat{U} , and \tilde{U} , defined on $(-\infty, \xi_w]$, (ξ_w, ξ_s) , and $[\xi_s, \infty)$, respectively. It follows from the analysis in Section 3 that the function $V(\xi)$ in (4.2)–(4.3) is well-defined and globally bounded on $\mathbb{R} \setminus \{\xi_s\}$, and continuous on each of the open intervals $(-\infty, \xi_w)$, (ξ_w, ξ_s) , (ξ_s, ∞) . The restrictions of V to these intervals are denoted V_k , V, and V, respectively.

The obvious approach to building the density profile is to use (4.2) to construct Ω -solutions corresponding to U_k , \hat{U} , and \tilde{U} , on their respective intervals of definition. Essentially, this is what we do, and we shall find that Ω , just like U, has a weak discontinuity (kink) at ξ_w , and a jump discontinuity at ξ_s .

However, as a first step in the analysis, we note that the situation is slightly more involved: according to the next lemma, for the Ω -variable there must necessarily be a discontinuity present also at the origin.

Lemma 4.1. If $\Omega(\xi)$ is a continuous solution of (4.2) on an open interval $I \subset (\xi_w, \xi_s)$ about the origin, then the corresponding density field $\rho(t, r)$ in (4.1) cannot satisfy requirement (C) in Section 1.

Proof. Assume for contradiction that requirement (C) is satisfied, i.e., $\rho(t,r)>0$ for all (t,r) with r>0 and $\frac{r}{t}\in I$. It then follows from (4.1), and $\mathrm{sgn}(t)=\mathrm{sgn}(\xi)$, that $\mathrm{sgn}(\Omega(\xi))=\mathrm{sgn}(\xi)$ for all $\xi\in I\setminus\{0\}$. As Ω is continuous at $\xi=0$, it follows that $\Omega(0)=0$. But then (4.2) implies that $\Omega(\xi)$ vanishes identically on I, which, according to (4.1), contradicts requirement (C). \square

We also observe from the previous proof that, as a consequence of requirement (*C*), the entire Ω -solution must satisfy $\operatorname{sgn}(\Omega(\xi)) = \operatorname{sgn}(\xi)$. In particular, by Lemma 4.1, the one-sided limit $\hat{\Omega}(0-)$ must be a strictly negative number.

So, differently from the three U-solutions U_k , \hat{U} , and \tilde{U} determined above, we now need to build four Ω -solutions, one on each of the intervals $(-\infty, \xi_w)$, $(\xi_w, 0)$, $(0, \xi_s)$, and (ξ_s, ∞) . To avoid introducing additional notation, we let $\hat{\Omega}(\xi)$ denote the Ω -solution on both of the intervals $(\xi_w, 0)$ and $(0, \xi_s)$, and refer to these as the left and right parts of $\hat{\Omega}$, respectively.

Since the function $V: \mathbb{R} \setminus \{\xi_s\} \to \mathbb{R}$ in (4.2) is bounded and continuous, the *existence* of solutions to (4.2) on each of the intervals $(-\infty, \xi_w)$, $(\xi_w, 0)$, $(0, \xi_s)$, (ξ_s, ∞) is unproblematic once an initial condition is prescribed at some finite point of the interval in question. While we shall utilize this fact, there remains two key issues: the Ω -solutions we build should satisfy the requirements (B) and (C) in Section 1; and, it should include a compressive discontinuity satisfying the Rankine–Hugoniot relation (2.12)₂ at $\xi = \xi$.

With these preparations, we proceed to construct the sought-for function $\Omega(\xi)$ according to the following steps.

4.1. Step 1: solving (4.2) on $[\xi_w, 0]$

We start by assigning any number $\Omega_0 < 0$, and solve (4.2), with $V(\xi) = \hat{V}(\xi)$, for $\hat{\Omega}(\xi)$ on $[\xi_{\rm w},0]$ with initial condition $\hat{\Omega}(0) = \Omega_0$. We note that Ω_0 is a free parameter, up to its sign. This "indeterminacy" reflects a special feature of the isothermal Euler system: whenever (ρ,\mathbf{u}) is a solution of (1.1)-(1.2)-(1.3), then so is $(\kappa\rho,\mathbf{u})$ for any $\kappa>0$.

4.2. Step 2: solving (4.2) on $(-\infty, \xi_w]$

We solve (4.2), with $V(\xi) = V_k(\xi)$, for $\Omega_k(\xi)$ on $(-\infty, \xi_w]$ with the initial condition $\Omega_k(\xi_w) = \hat{\Omega}(\xi_w)$, where the latter value is obtained from Step 1. Since $V_k'(\xi_w) \neq \hat{V}'(\xi_w)$ while $V_k(\xi_w) = \hat{V}(\xi_w)$, it follows from (4.2) that also $\Omega_k'(\xi_w) \neq \hat{\Omega}'(\xi_w)$; i.e., the Ω -solution inherits a kink from the U-solution at this point.

As noted above, the existence of $\Omega_k(\xi)$ is unproblematic on the whole interval $(-\infty, \xi_w]$. However, to address requirement (B) we shall need more precise information about the behavior of $\Omega_k(\xi)$ as $\xi \downarrow -\infty$, which corresponds to the behavior of $\rho(t,r)$ as $t \uparrow 0$ at a fixed location r > 0. We have:

Lemma 4.2. The solution $\Omega_k(\xi)$ to (4.2) on $(-\infty, \xi_w]$ satisfies

$$\lim_{\xi \downarrow -\infty} \frac{\Omega_{\mathbf{k}}(\xi)}{|\xi|^{\beta}} = C_{-},\tag{4.4}$$

for a finite, negative constant C_- . As a consequence, the corresponding density field $\rho(t,r)$ given by (4.1) satisfies

$$\lim_{t \to 0} \rho(t, r) = -C_{-}r^{\beta} \quad \text{at each fixed location } r > 0.$$
 (4.5)

Proof. We first argue that the function $V_k(\xi) = -\frac{1}{a^2}(U_k(\xi) - \xi)U_k'(\xi)$ satisfies

$$|V_{k}(\xi) - \frac{\beta}{\xi}| \le \frac{C}{\xi^{2}} \quad \text{for } \xi \in (-\infty, \xi_{w}], \tag{4.6}$$

for some constant *C*. Since $V_k(\xi)$ is bounded on $(-\infty, \xi_w]$, to verify (4.6) it suffices to show that the quantity

$$\xi^2 |V_k(\xi) - \frac{\beta}{\varepsilon}|$$
 remains bounded as $\xi \downarrow -\infty$. (4.7)

For this we use (4.3) to write

$$\xi^{2}|V_{k}(\xi) - \frac{\beta}{\xi}| = \xi^{2} \left| \frac{(U_{k}(\xi) - \xi)(\beta\xi + mU_{k}(\xi))}{\xi((U_{k}(\xi) - \xi)^{2} - a^{2})} + \frac{\beta}{\xi} \right|
= |\xi| \left| \frac{(m + \beta)\xi U_{k}(\xi) - (m + \beta)U_{k}(\xi)^{2} + \beta a^{2}}{(U(\xi) - \xi)^{2} - a^{2}} \right|.$$
(4.8)

Sending $\xi \downarrow -\infty$ in (4.8) and using Lemma 3.5, yield (4.7), and thus (4.6).

Next, writing (4.2) in the form

$$\frac{\Omega'_{\mathbf{k}}(\xi)}{\Omega_{\mathbf{k}}(\xi)} = \frac{\beta}{\xi} + (V_{\mathbf{k}}(\xi) - \frac{\beta}{\xi}),$$

and integrating from $\xi < \xi_w$ to ξ_w , yield

$$\frac{\Omega_{\mathbf{k}}(\xi)}{|\xi|^{\beta}} = \frac{\Omega_{\mathbf{w}}}{|\xi_{\mathbf{w}}|^{\beta}} \cdot \exp\left[\int_{\xi}^{\xi_{\mathbf{w}}} \frac{\beta}{\eta} - V_{\mathbf{k}}(\eta) \, d\eta\right],$$

where $\Omega_w := \Omega_k(\xi_w) < 0$. Sending $\xi \downarrow -\infty$ yields (4.4) with

$$C_{-} = \frac{\Omega_{\mathrm{w}}}{|\xi_{\mathrm{w}}|^{\beta}} \cdot \exp\left[\int_{-\infty}^{\xi_{\mathrm{w}}} \frac{\beta}{\eta} - V_{\mathrm{k}}(\eta) \, d\eta\right] < 0,$$

which is finite according to (4.6). Finally, applying this in (4.1) we obtain, for any fixed location r > 0,

$$\lim_{t \uparrow 0} \rho(t, r) = \lim_{t \uparrow 0} \operatorname{sgn}(t)|t|^{\beta} \Omega_{k}(\frac{r}{t})$$

$$= -r^{\beta} \cdot \left(\lim_{\xi \downarrow -\infty} \frac{\Omega_{k}(\xi)}{|\xi|^{\beta}}\right) = -C_{-}r^{\beta}, \tag{4.9}$$

verifying (4.5). \square

Remark 4.1. We note that, since $\beta < 0$, (4.5) shows that the density field suffers blowup at the center of motion at time t = 0.

4.3. Step 3: solving (4.2) on $[\xi_s, +\infty)$

It follows from Lemma 4.2 and requirement (B) in Section 1 that the density field we seek should satisfy

$$\lim_{t\downarrow 0} \rho(t,r) = -C_{-}r^{\beta} \qquad \text{for each } r > 0. \tag{4.10}$$

We use this condition to select the appropriate solution $\tilde{\Omega}(\xi)$ of (4.2) on $[\xi_s, +\infty)$. This is most easily done by repeating the argument in the proof of Lemma 4.2. We first write (4.2) on $[\xi_s, +\infty)$ in the form

$$\frac{\tilde{\Omega}'(\xi)}{\tilde{\Omega}(\xi)} = \frac{\beta}{\xi} + (\tilde{V}(\xi) - \frac{\beta}{\xi}),\tag{4.11}$$

and observe that, as in the proof above, there is a constant $\mathcal C$ such that

$$|\tilde{V}(\xi) - \frac{\beta}{\xi}| \le \frac{C}{\xi^2}$$
 for $\xi \in [\xi_s, +\infty)$. (4.12)

Integrating (4.11) from ξ_s we obtain that

$$\frac{\tilde{\Omega}(\xi)}{\xi^{\beta}} = \frac{\tilde{\Omega}(\xi_{s})}{\xi_{s}^{\beta}} \cdot \exp\left[\int_{\xi_{s}}^{\xi} \tilde{V}(\eta) - \frac{\beta}{\eta} d\eta\right]. \tag{4.13}$$

Thanks to (4.12), we can now define

$$\tilde{\Omega}(\xi_{s}) := -C_{-} \cdot \xi_{s}^{\beta} \cdot \exp\left[\int_{\xi_{-}}^{\infty} \frac{\beta}{\eta} - \tilde{V}(\eta) \, d\eta\right], \tag{4.14}$$

where $C_- < 0$ is given by (4.4). This selects a unique solution of $\tilde{\Omega}(\xi)$ of (4.2) on $[\xi_s, +\infty)$, which, according to (4.13) and (4.14), satisfies

$$\lim_{\xi \uparrow +\infty} \frac{\tilde{\Omega}(\xi)}{\xi^{\beta}} = -C_{-}. \tag{4.15}$$

Finally, in terms of (4.1) with $\Omega = \tilde{\Omega}$, this gives

$$\begin{split} \lim_{t\downarrow 0} \rho(t,r) &= \lim_{t\downarrow 0} \ t^\beta \tilde{\varOmega}(\frac{r}{t}) \\ &= -C_- r^\beta \qquad \text{at any fixed location } r>0. \end{split} \tag{4.16}$$

Thus, requirement (B) in Section 1 selects a unique Ω -solution for continuing the density field $\rho(t, r)$ across t = 0.

4.4. Step 4: solving (4.2) on $(0, \xi_s]$

The solution $\tilde{\Omega}(\xi)$ constructed in the previous step provides the value $\tilde{\Omega}(\xi_s)$ at the immediate outside of the expanding shockwave which is to propagate along $r=\xi_s t$. Applying the Rankine–Hugoniot condition $(2.12)_2$ with $\tilde{\xi}=\xi_s$, $U_+=\tilde{U}(\xi_s)$, $\Omega_+=\tilde{\Omega}(\xi_s)$, and $\Omega_-=\hat{\Omega}(\xi_s)$, yields

$$\hat{\Omega}(\xi_{\rm S}) = \frac{(\xi_{\rm S} - \tilde{U}(\xi_{\rm S}))^2}{a^2} \tilde{\Omega}(\xi_{\rm S}). \tag{4.17}$$

The latter value provides the initial data at $\xi = \xi_s$ for the solution $\hat{\Omega}(\xi)$ of (4.2) on $(0, \xi_s)$. As noted above, since $\hat{V}(\xi)$ is bounded on $(0, \xi_s]$, it is unproblematic to integrate (4.2) there.

Finally, let us verify that the resulting shock is compressive. It follows from (3.15) that $\tilde{U}(\xi_s) < \xi_s < \xi_s - a$, so that: (a) the fluid crosses the expanding shock from its outside to its inside, and (b) $(\xi_s - \tilde{U}(\xi_s))^2 > a^2$. Using (b) in (4.17) yields $\hat{\Omega}(\xi_s) > \tilde{\Omega}(\xi_s)$, so that (via (1.8)₁) the density of the fluid is higher on the immediate inside of the shock, compared to on the immediate outside. Thus, the density of a fluid particle increases as it passes through the shock, and the shock is compressive.

This concludes the construction of the function $\Omega(\xi)$ to be used for defining the density in radial similarity flows for isother-

mal Euler; see Fig. 2. We sum up the properties of the resulting density field in the following proposition.

Proposition 4.3. For space dimensions n=2 or n=3, let $\beta \in (1-n,\frac{1-n}{2})$. Consider the solutions Ω_k , $\hat{\Omega}$, $\tilde{\Omega}$ of the similarity ODE (4.2) constructed above by using the parameter $\Omega_0 < 0$ and the solutions U_k , \hat{U} , \tilde{U} of the similarity ODE (3.1). Finally, let the values $\xi_w < 0$ and $\xi_s > 0$ be determined as in (3.6) and in Section 3.5, respectively. Define the functions $\rho(t,r)$ and $\Omega(\xi)$ by

$$\rho(t,r) = \operatorname{sgn}(t)|t|^{\beta} \Omega(\frac{r}{t}) := \begin{cases} -|t|^{\beta} \Omega_{k}(\frac{r}{t}) & -\infty < \frac{r}{t} \le \xi_{w} \\ -|t|^{\beta} \hat{\Omega}(\frac{r}{t}) & \xi_{w} \le \frac{r}{t} < 0 \\ t^{\beta} \hat{\Omega}(\frac{r}{t}) & 0 < \frac{r}{t} < \xi_{s} \\ t^{\beta} \hat{\Omega}(\frac{r}{t}) & \xi_{s} < \frac{r}{t} < \infty, \end{cases}$$

$$(4.18)$$

together with

$$\rho(0,r) := -C_{-}r^{\beta},\tag{4.19}$$

where $C_- < 0$ is given by Lemma 4.2. Then $\Omega(\xi)$ is globally bounded and (4.18)–(4.19) yield a density field $\rho(t,r)$ in which a weak discontinuity converges toward the origin along $r = \xi_w t$ for t < 0, and a compressive jump discontinuity, satisfying the Rankine–Hugoniot jump condition in (2.11)₂, diverges from the origin along $r = \xi_s t$ for t > 0. The function $r \mapsto \rho(t,r)$ is bounded at each time $t \neq 0$. Finally, ρ satisfies the physical requirements (B) and (C) in Section 1.

Proof. The presence of the weak discontinuity and the jump discontinuity follows by construction, as do the boundedness of $r \mapsto \rho(t,r)$ at times $t \neq 0$. Also, as detailed in Section 4.3, requirements (B) is satisfied by construction. Compressibility was argued for above. It remains to argue for requirement (C), i.e., $\rho(t,r)$ is positive almost everywhere. According to (4.18) it suffices to verify that

$$\Omega(\xi) \geqslant 0$$
 when $\xi \geqslant 0$, respectively. (4.20)

Observing that continuous solutions of (4.2) cannot change sign, we consider each of the subintervals $[\xi_w,0)$, $(-\infty,\xi_w]$, (ξ_s,∞) , and $(0,\xi_s)$ in turn. First, from Section 4.1, $\Omega_0<0$ provides initial data for $\hat{\Omega}$ at $\xi=0$. Thus, $\hat{\Omega}$ is negative on $[\xi_w,0)$. In particular, the initial data $\Omega_k(\xi_w):=\hat{\Omega}(\xi_w)$ is negative, and it follows that $\Omega_k(\xi)<0$ for all $\xi\in(-\infty,\xi_w]$. Next, recall that the constant C_- given by Lemma 4.2 is negative. It follows from (4.16) that $\tilde{\Omega}(\xi)$ must be positive on $[\xi_s,\infty)$. Finally, according to (4.17), the initial value $\hat{\Omega}(\xi_s)$ for $\hat{\Omega}$ on $(0,\xi_s]$ is then also positive, and it follows that $\hat{\Omega}(\xi)>0$ throughout $(0,\xi_s]$. This completes the proof of (4.20), and requirement (C) follows. \square

5. Weak and radial weak Euler solutions

It remains to verify that the functions $\rho(t,r)$ and u(t,r) given by Propositions 3.7 and 4.3 provide genuine, weak solutions to the original, multi-d isothermal Euler system (1.1)–(1.2). The argument for this is detailed in Section 6. However, we first define exactly what is meant by a weak solution to the Euler system: first for general, multi-d solutions, and then specialized to the case of radial solutions. The relationship between these is given by Proposition 5.4. We formulate the definitions at the level of general barotropic flows, specializing to isothermal flows in Section 6.

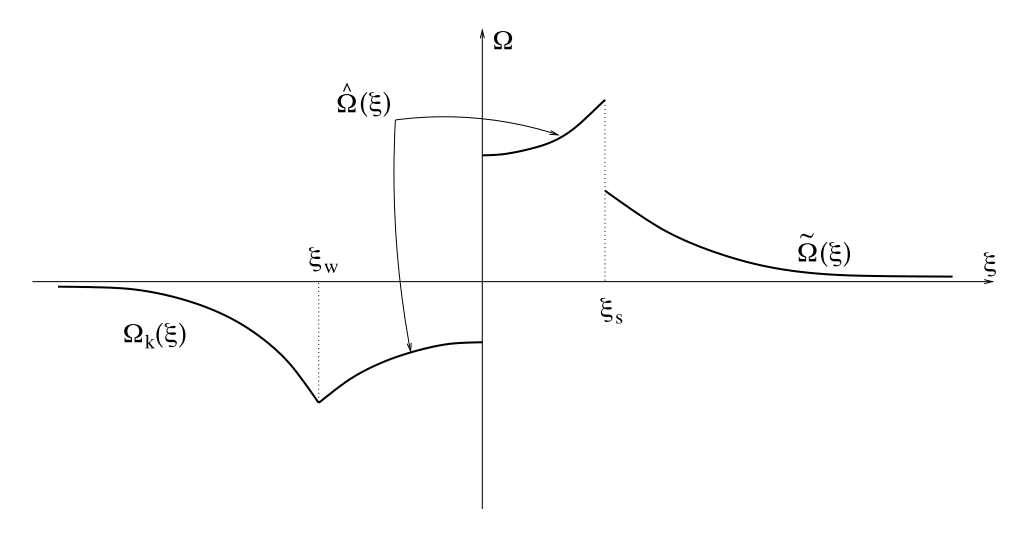


Fig. 2. Complete $\Omega(\xi)$ -profile (schematic).

5.1. Multi-d weak solutions

We write $\rho(t)$ for $\rho(t,\cdot)$ etc., $\mathbf{u}=(u_1,\ldots,u_n)$, $u:=|\mathbf{u}|$, and let $\mathbf{x}=(x_1,\ldots,x_n)$ denote the spatial variable in \mathbb{R}^n , while $r=|\mathbf{x}|$ varies over $\mathbb{R}^+_0=[0,\infty)$.

Definition 5.1. Consider the compressible, barotropic Euler system (1.1)–(1.2) in n space dimensions with a given pressure function $p=p(\rho)\geq 0$. Then the measurable functions $\rho,\,u_1,\ldots,u_n:\mathbb{R}_t\times\mathbb{R}_{\mathbf{x}}^n\to\mathbb{R}$ constitute a weak solution to (1.1)–(1.2) provided that:

- (1) the maps $t \mapsto \rho(t)$ and $t \mapsto \rho(t)u(t)$ belong to $C^0(\mathbb{R}_t; L^1_{loc}(\mathbb{R}^n_t))$;
- (2) the functions ρu^2 and $p(\rho)$ belong to $L^1_{loc}(\mathbb{R}_t \times \mathbb{R}_x^n)$;
- (3) the conservation laws for mass and momentum are satisfied weakly in sense that

$$\int_{\mathbb{R}} \int_{\mathbb{R}^n} \rho \varphi_t + \rho \mathbf{u} \cdot \nabla_{\mathbf{x}} \varphi \, d\mathbf{x} dt = 0$$
 (5.1)

and

$$\int_{\mathbb{R}} \int_{\mathbb{R}^n} \rho u_i \varphi_t + \rho u_i \mathbf{u} \cdot \nabla_{\mathbf{x}} \varphi + p(\rho) \varphi_{x_i} \, d\mathbf{x} dt = 0 \qquad \text{for } i = 1, \dots, n,$$
(5.2)

whenever $\varphi \in C^1_c(\mathbb{R}_t \times \mathbb{R}^n_{\mathbf{x}})$ (the set of C^1 functions with compact support).

Remark 5.1. In this definition, condition (1) guarantees that the conserved quantities define continuous maps into $L^1_{loc}(\mathbb{R}^n_{\mathbf{x}})$, which is the natural function space in this setting. Taken together, conditions (1) and (2) ensure that all terms occurring in the weak formulations (5.1) and (5.2) are locally integrable in space and time.

5.2. Radial weak solutions

We next rewrite Definition 5.1 for radial solutions. For this we use the following notation. As above m := n - 1 and we set

$$\mathbb{R}^+ = (0, \infty), \qquad \mathbb{R}_0^+ = [0, \infty),$$

$$L^1_{(loc)}(dt \times r^m dr) = L^1_{(loc)}(\mathbb{R} \times \mathbb{R}_0^+, dt \times r^m dr).$$

Definition 5.2. With the notation introduced above, $C_c^1(\mathbb{R} \times \mathbb{R}_0^+)$ denotes the set of real-valued functions $\psi: \mathbb{R} \times \mathbb{R}_0^+ \to \mathbb{R}$ that are C^1 smooth on $\mathbb{R} \times \mathbb{R}_0^+$ and vanishes outside $[-\bar{t}, \bar{t}] \times [0, \bar{r}]$ for some $\bar{t}, \bar{r} \in \mathbb{R}^+$. Also, $C_0^1(\mathbb{R} \times \mathbb{R}_0^+)$ denotes the set of those functions $\theta \in C_c^1(\mathbb{R} \times \mathbb{R}_0^+)$ with the additional property that $\theta(t, 0) \equiv 0$.

Using these function classes, the weak formulation of the multi-d Euler system (1.1)-(1.2), for radial solutions, takes the following form.

Definition 5.3. Consider the radial version (1.4)–(1.5) of the compressible Euler system (1.1)–(1.2) with a given pressure function $p = p(\rho) \ge 0$. Then the measurable functions ρ , $u : \mathbb{R}_t \times \mathbb{R}_t^+ \to \mathbb{R}$ constitute a *radial weak solution* to (1.4)–(1.5) provided that:

- (i) the maps $t \mapsto \rho(t)$ and $t \mapsto \rho(t)u(t)$ belong to $C^0(\mathbb{R}_t; L^1_{loc}(r^m dr))$:
- (ii) the functions ρu^2 and $p(\rho)$ belong to $L^1_{loc}(dt \times r^m dr)$;
- (iii) the conservation laws for mass and momentum are satisfied in the sense that

$$\int_{\mathbb{R}} \int_{\mathbb{R}^{+}} (\rho \psi_{t} + \rho u \psi_{r}) r^{m} dr dt = 0 \qquad \forall \psi \in C_{c}^{1}(\mathbb{R} \times \mathbb{R}_{0}^{+})$$

$$\int_{\mathbb{R}} \int_{\mathbb{R}^{+}} \left(\rho u \theta_{t} + \rho u^{2} \theta_{r} + p(\rho) \left(\theta_{r} + \frac{m\theta}{r} \right) \right) r^{m} dr dt = 0$$

$$\forall \theta \in C_{0}^{1}(\mathbb{R} \times \mathbb{R}_{0}^{+}).$$
(5.4)

We now have:

Proposition 5.4. Assume that $(\rho(t,r), u(t,r))$ is a radial weak solution of (1.4)–(1.5) according to Definition 5.3, and define the functions

$$\rho(t, \mathbf{x}) := \rho(t, r), \qquad \mathbf{u}(t, \mathbf{x}) := u(t, r) \frac{\mathbf{x}}{r}. \tag{5.5}$$

Then $(\rho(t, \mathbf{x}), \mathbf{u}(t, \mathbf{x}))$ is a weak solution of the multi-d system (1.1)-(1.2) according to Definition 5.1.

Proof. This result was proved by Hoff ([20], Theorem 5.7) in the setting of the isothermal Navier–Stokes system; the same argument applies to the Euler system. \Box

6. Radial converging-diverging similarity solutions as weak solutions

In this section we return to isothermal flow $(p(\rho) = a^2 \rho)$ and the radial converging-diverging similarity solutions u(t,r), $\rho(t,r)$ constructed in Sections 3 and 4. The goal is to establish properties (i), (ii), and (iii) in Definition 5.3 for these solutions, and we first consider the integrability and continuity requirements in (i) and (ii). The weak forms of the equations are then treated in Section 6.2.

6.1. Integrability and continuity

Lemma 6.1. Assume that $\beta \in (1-n, \frac{1-n}{2})$ for n=2 or n=3, and the isothermal pressure law $p(\rho)=a^2\rho$. Then the density field $\rho(t,r)$ and the velocity field u(t,r) given by Propositions 3.7 and 4.3, respectively, satisfy parts (i) and (ii) of Definition 5.3.

Proof. We first claim that ρ maps into $L^1_{loc}(r^m dr)$, i.e., for any $\bar{r} > 0$ and for any $t \in \mathbb{R}$, we have

$$\int_0^{\bar{r}} \rho(t, r) r^m \, dr < \infty. \tag{6.1}$$

According to Proposition 4.3 the function $r\mapsto \rho(t,r)$ is bounded at all times $t\neq 0$. Thus, the only issue is at time t=0, where $\rho(0,r)=-C_-r^\beta$ according to (4.19). Since, by assumption, $-m=1-n<\beta$, we have $\beta+m>0$, so that (6.1) is satisfied also at time 0.

Since the velocity u(t, r) given by Proposition 3.7 is globally bounded, it follows that also ρu belongs to $L^1_{loc}(r^m dr)$ at all times.

Next, consider the continuity of $t\mapsto \rho(t)$. For concreteness fix a time t>0, so that for any $\tau>0$,

$$\begin{split} \|\rho(t) - \rho(\tau)\|_{L^1([0,\bar{r}],r^m dr)} &= \int_0^{\bar{r}} |\rho(t,r) - \rho(\tau,r)| r^m dr \\ &= \int_0^{\bar{r}} |t^\beta \Omega(\frac{r}{t}) - \tau^\beta \Omega(\frac{r}{\tau})| r^m dr. \end{split}$$

Since Ω is a bounded function and almost everywhere continuous, it follows from the dominated convergence theorem that $\|\rho(t)-\rho(\tau)\|_{L^1([0,\bar{r}],r^mdr)}\to 0$ as $\tau\to t$. For t=0 we have, according to (4.19), that

$$\|\rho(0) - \rho(\tau)\|_{L^1([0,\bar{r}],r^m dr)} = \int_0^{\bar{r}} |C_- r^\beta + \tau^\beta \Omega(\frac{r}{\tau})| r^m dr.$$
 (6.2)

Consider first the case when $\tau \downarrow 0$. Then, for a fixed r>0 and for $0<\tau<\frac{r}{\xi_s}$, the integrand in (6.2) is given by (4.18) as

$$|C_{-}r^{\beta} + \tau^{\beta}\tilde{\Omega}(\frac{r}{\tau})|r^{m}. \tag{6.3}$$

Substituting for $\tilde{\Omega}$ from (4.13) we obtain

$$|C_{-}r^{\beta} + \tau^{\beta} \tilde{\Omega}(\frac{r}{\tau})|r^{m} = \left|C_{-} + \frac{\tilde{\Omega}(\xi_{s})}{\xi_{s}^{\beta}} \cdot \exp\left[\int_{\xi_{s}}^{\frac{r}{\tau}} \tilde{V}(\eta) - \frac{\beta}{\eta} d\eta\right]\right| r^{\beta+m}.$$

From (4.12) it follows that the last expression is bounded by a constant times $r^{\beta+m}$ for τ near zero. As $\beta+m>0$ by assumption, this shows that the integrand in (6.2) is bounded by a fixed $L^1([0,\bar{r}],dr)$ function. Finally, for each fixed r>0, the integrand (6.3) tends to zero as $\tau\downarrow 0$ according to (4.16). The dominated convergence theorem thus gives that $\|\rho(0)-\rho(\tau)\|_{L^1([0,\bar{r}],r^mdr)}\to 0$ as $\tau\downarrow 0$. A similar argument applies for $\tau\uparrow 0$, establishing continuity of $t\mapsto \rho(t)$ as a map into $L^1_{loc}(r^mdr)$. Also, since $u(t,r)=U(\frac{r}{t})$, with $U(\xi)$ globally bounded and almost everywhere continuous, the argument for the continuity of $t\mapsto \rho(t)u(t)$ is essentially the same as that for $t\mapsto \rho(t)$; we omit the details. This establishes part (i) of Definition 5.3.

Finally, since the pressure $p(\rho)$ is linear in ρ and u is globally bounded, Part (ii) follows directly from part (i). \square

For later use we record the following direct consequence of the previous lemma.

Corollary 6.2. For $\bar{r} > 0$ let

$$M(t; \bar{r}) := \int_0^{\bar{r}} \rho(t, r) r^m dr, \qquad I_q(t; \bar{r}) := \int_0^{\bar{r}} \rho(t, r) |u(t, r)|^q r^m dr$$
for $q = 1, 2$.

Then, under the assumptions of Lemma 6.1, the maps $t \mapsto M(t; \bar{r})$, $t \mapsto I_1(t; \bar{r})$, and $t \mapsto I_2(t; \bar{r})$ are continuous at all times $t \in \mathbb{R}$.

6.2. Weak form of the equations

Lemma 6.3. Under the assumptions of Lemma 6.1 the density field $\rho(t,r)$ and the velocity field u(t,r) given by Propositions 3.7 and 4.3, respectively, satisfy part (iii) of Definition 5.3.

Proof. We exploit that the local integrability properties in parts (i) and (ii) of Definition 5.3 have been verified, and specifically that Corollary 6.2 applies. The issue will then reduce to estimating the fluxes of the conserved quantities across spheres of vanishing radii.

We fix $\psi \in C_c^1(\mathbb{R} \times \mathbb{R}_0^+)$ and $\theta \in C_0^1(\mathbb{R} \times \mathbb{R}_0^+)$ with supp ψ , supp $\theta \subset [-T,T] \times [0,\bar{r}]$ (recall Definition 5.2). As in Definition 5.3, ψ and θ will be test functions for the mass and momentum equations (5.3) and (5.4), respectively. Next, for any $\delta < \min(T\xi_s, T|\xi_w|, \bar{r})$, we define the open regions

$$J_{\delta} = \left\{ (t, r) \mid -T < t < T, \ \delta < r < \overline{r}, \ \frac{t}{r} < \frac{1}{\xi_{s}} \right\},$$

and

$$K_{\delta} = \left\{ (t,r) \mid -T < t < T, \; \delta < r < \bar{r}, \; \frac{t}{r} > \frac{1}{\xi_{s}} \right\},$$

(see Fig. 3), and set

$$M(\psi) := \iint_{\mathbb{R} \times \mathbb{R}^+} (\rho \psi_t + \rho u \psi_r) r^m dr dt$$

$$= \left\{ \iint_{\mathbb{R} \times [0, \delta]} + \iint_{J_{\delta}} + \iint_{K_{\delta}} \right\} (\rho \psi_t + \rho u \psi_r) r^m dr dt$$

$$=: M_{\delta}(\psi) + \left\{ \iint_{L} + \iint_{K_{\delta}} \right\} (\rho \psi_t + \rho u \psi_r) r^m dr dt \qquad (6.4)$$

and

$$I(\theta) := \iint_{\mathbb{R} \times \mathbb{R}^{+}} \left(\rho u \theta_{t} + \rho u^{2} \theta_{r} + p \left(\theta_{r} + \frac{m \theta}{r} \right) \right) r^{m} dr dt$$

$$= \left\{ \iint_{\mathbb{R} \times [0, \delta]} + \iint_{J_{\delta}} + \iint_{K_{\delta}} \right\}$$

$$\times \left(\rho u \theta_{t} + \rho u^{2} \theta_{r} + p \left(\theta_{r} + \frac{m \theta}{r} \right) \right) r^{m} dr dt$$

$$=: I_{\delta}(\theta) + \left\{ \iint_{J_{\delta}} + \iint_{K_{\delta}} \right\}$$

$$\times \left(\rho u \theta_{t} + \rho u^{2} \theta_{r} + p \left(\theta_{r} + \frac{m \theta}{r} \right) \right) r^{m} dr dt. \tag{6.5}$$

We shall verify the claim of the lemma by verifying that $M(\psi)$ and $I(\theta)$ vanish. This is carried out in the following by showing that the right hand sides of (6.4) and (6.5) vanish as $\delta \downarrow 0$.

We first note that the continuity of the maps $t\mapsto M(t;\bar{r})$, $t\mapsto I_1(t;\bar{r})$, and $t\mapsto I_2(t;\bar{r})$, which was established above, implies the local $r^m dr dt$ -integrability of $\rho, p \propto \rho$, ρu , and ρu^2 . As a consequence, both $M_\delta(\psi)$ and $I_\delta(\theta)$ tend to zero as $\delta \downarrow 0$. (Note that for $I_\delta(\theta)$, we make use of the fact that θ belongs to the space $C_0^1(\mathbb{R}\times\mathbb{R}_0^+)$; in particular, $\frac{m}{r}$ is a globally bounded function.)

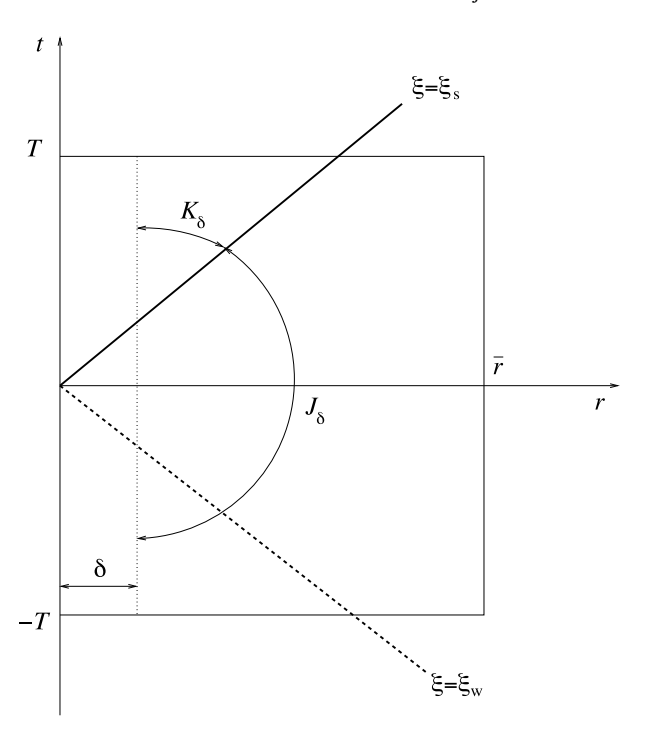


Fig. 3. Regions of integration in the weak formulation.

It remains to estimate the integrals over J_{δ} and K_{δ} in (6.4) and (6.5). For this we first recall that (ρ , u), by construction, is a classical (Lipschitz continuous) solution of the isothermal Euler system (1.4)–(1.5) within each of the open regions J_{δ} and K_{δ} , and that the Rankine–Hugoniot relations (2.5)–(2.6), with $\dot{\mathcal{R}}=\xi_{\rm s}$, are satisfied across their common boundary along the straight line $r=\xi_{\rm s}t$. Applying the divergence theorem to each region we therefore have,

$$\left\{ \iint_{J_{\delta}} + \iint_{K_{\delta}} \right\} (\rho \psi_t + \rho u \psi_r) \ r^m dr dt = \delta^m \int_{-T}^{T} (\rho u \psi)(t, \delta) dt$$
(6.6)

and

$$\left\{ \iint_{J_{\delta}} + \iint_{K_{\delta}} \left\{ \left(\rho u \theta_{t} + \rho u^{2} \theta_{r} + p \left(\theta_{r} + \frac{m \theta}{r} \right) \right) r^{m} dr dt \right\} \\
= \delta^{m} \int_{-T}^{T} \left[\left(\rho u^{2} + p \right) \theta \right] (t, \delta) dt. \tag{6.7}$$

The goal is to show that the terms on the right-hand sides of (6.6) and (6.7) both tend to zero as $\delta \downarrow 0$. Since the velocity u(t,r) is globally bounded, ψ and θ are bounded functions, and $p \propto \rho$, it suffices to show that the quantity $\delta^m \int_{-T}^T \rho(t,\delta) dt$ tends to zero with δ . Using (4.18) and switching to ξ as integration variable, we have

$$\delta^{m} \int_{-T}^{T} \rho(t,\delta) dt = \delta^{n+\beta} \left\{ \int_{-\infty}^{\xi_{w}} + \int_{\xi_{w}}^{-\delta/T} + \int_{\delta/T}^{\xi_{s}} + \int_{\xi_{s}}^{\infty} \right\} \frac{|\Omega(\xi)|}{|\xi|^{\beta+2}} d\xi$$

$$= \delta^{n+\beta} \left\{ \int_{-\infty}^{\xi_{w}} \frac{|\Omega_{k}(\xi)|}{|\xi|^{\beta+2}} d\xi + \int_{\xi_{w}}^{-\delta/T} \frac{|\hat{\Omega}(\xi)|}{|\xi|^{\beta+2}} d\xi + \int_{\delta/T}^{\xi_{s}} \frac{\hat{\Omega}(\xi)}{\xi^{\beta+2}} d\xi + \int_{\xi_{s}}^{\infty} \frac{\tilde{\Omega}(\xi)}{\xi^{\beta+2}} d\xi \right\}. \tag{6.8}$$

According to (4.4) and (4.15), we have, for a suitable constant C, $|\Omega_k(\xi)| \le C|\xi|^{\beta}$ for $\xi < \xi_w$, and $\tilde{\Omega}(\xi) \le C\xi^{\beta}$ for $\xi > \xi_s$,

Using these bounds in (6.8), together with the boundedness of $\hat{\Omega}$ and the assumption that $\beta \in (1 - n, \frac{1 - n}{2})$, we obtain

$$\delta^m \int_{-T}^{T} \rho(t,\delta) dt \leq const. \delta^{n+\beta} (1 + \frac{1}{\delta^{\beta+1}}),$$

so that

$$\lim_{\delta \downarrow 0} \delta^m \int_{-T}^T \rho(t,\delta) dt = 0.$$

As noted above, this implies that the integrals in (6.6) and (6.7) tend to zero as $\delta \downarrow 0$. This concludes the proof that (ρ, u) satisfies part (iii) of Definition 5.3. \Box

We summarize our findings in the following theorem.

Theorem 6.4. Consider the radial, isothermal Euler system (1.4)–(1.5) with pressure function $p = a^2 \rho$ in n = 2 or n = 3 space dimensions. Fix any numbers $\beta \in (1 - n, \frac{1-n}{2})$ and $\Omega_0 < 0$.

dimensions. Fix any numbers $\beta \in (1-n, \frac{1-n}{2})$ and $\Omega_0 < 0$. Then there exists a radial weak solution $(\rho(t, r), u(t, r))$ to (1.4)–(1.5), in the sense of Definition 5.3, of similarity type

$$\rho(t,r) = \operatorname{sgn}(t)|t|^{\beta} \Omega(\xi), \qquad u(t,r) = U(\xi), \qquad \xi = \frac{r}{t},$$

where $U(\xi)$ and $\Omega(\xi)$ are as described by Propositions 3.7 and 4.3, respectively. In particular, the following holds:

- (1) The functions $U(\xi)$ and $\Omega(\xi)$ are globally bounded and approach limits $U^* < 0$ and 0, respectively, as $|\xi| \to \infty$; $U(\xi)$ and $\Omega(\xi)$ have a weak discontinuity at $\xi = \xi_w < 0$ (determined by (3.6)) and a jump discontinuity at $\xi = \xi_s > 0$ (determined in Section 3.5); $\Omega(\xi)$ has a jump discontinuity also at $\xi = 0$, with $\Omega(0-) = \Omega_0$.
- (2) The resulting solution $(\rho(t,r), u(t,r))$ describes a flow in which a weak discontinuity converges toward the origin along the straight path $r = \xi_w t$ for t < 0, an infinite density (and thus pressure) is generated at the origin r = 0 at time t = 0, and an outgoing shock emerges and propagates along the straight path $r = \xi_s t$ for t > 0.
- (3) The density and velocity profiles at time t=0 are given by

$$\rho(0, r) = Cr^{\beta}, \qquad u(0, r) \equiv U^*,$$

where C is a positive constant.

- (4) The emerging shock wave is compressive: as fluid passes through the shock, its density increases.
- (5) The flow satisfies the requirements (A), (B), and (C) in Section 1.

Finally, any such solution provides a weak solution

$$\rho(t, \mathbf{x}) := \rho(t, |\mathbf{x}|), \qquad \mathbf{u}(t, \mathbf{x}) := u(t, |\mathbf{x}|) \frac{\mathbf{x}}{|\mathbf{x}|}$$
(6.9)

of the multi-d isothermal system (1.1)-(1.2), according to Definition 5.1.

Proof. The properties (1)-(5) hold according to Propositions 3.7 and 4.3. Lemmas 6.1 and 6.3 show that (ρ, u) is a weak radial solution of (1.4)-(1.5). Finally, Proposition 5.4 shows that the density and velocity fields given by (6.9) define a weak solution of (1.1)-(1.2) according to Definition 5.1. \Box

7. Additional remarks

We collect some further properties of the radial similarity solutions constructed above. In the following we fix a radial weak solution of the type described by Theorem 6.4.

First, consider the behavior of characteristics $\dot{r} = u \pm a$ and particle trajectories $\dot{r} = u$ in the constructed solutions.

We first note that the only possibility for a path of the form $r = \bar{\xi}t$ (with $\bar{\xi}$ constant) to be a characteristic for the type of flow described by Theorem 6.4, is for $\bar{\xi} = \xi_w$, in which case it is a 1-characteristic. (This follows, since the graph of $\xi \mapsto U(\xi)$, where U is given by Proposition 3.7, intersects the straight line $U = \xi + a$ if and only if $\xi = \xi_w$, while it does not intersect the line $U = \xi - a$; see Fig. 1.) Indeed, the path $r = \xi_W t$ is the "critical" 1-characteristic in the lower half of the (r, t)-plane in the following sense. If r = c(t) is a 1-characteristic which at some time \bar{t} < 0 is located inside of $r = \xi_W t$ (i.e., $c(\bar{t}) < \xi_W \bar{t}$), then r = c(t)reaches the center of motion r = 0 at some strictly negative time. On the other hand, if r = c(t) is any 1-characteristic which at some time $\bar{t} < 0$ is located outside of $r = \xi_w t$, then it crosses the r-axis at a strictly positive location (i.e., c(0) > 0), with the speed $U^* - a$, and subsequently disappears at some positive time into the expanding shock wave propagating along $r = \xi_s t$.

Also, all particle trajectories cross the critical characteristic from below (in the (r, t)-plane) and proceed to cross the r-axis with the common speed U^* < 0. It follows that there is no "accumulation" of particles at the center of motion; in particular, the trivial particle trajectory $r(t) \equiv 0$ is the unique one passing through the origin. Consequently, the density $\rho(t,r)$ does not "contain a Dirac delta" at time of collapse. (Solutions of "cumulative" type where all, or part, of the mass accumulates at the origin, were considered in [2,21]. However, a rigorous analysis of such solutions would require a more general notion of weak solutions than the one employed in the present work.)

Next, recall from Lemma 6.1 that the mass is locally finite at all times: any ball of finite radius contains only a finite amount of mass at any time, including t = 0. Although the density $\rho(t, r)$ decays to zero at any fixed time t as $r \uparrow \infty$, this decay is too slow to give bounded total mass: the mass density $\rho(t, r)r^m$ grows like $r^{\beta+m}$ for t fixed as $r \uparrow \infty$, and the assumption $\beta+m>0$ yields unbounded total mass. Since the velocity u(t, r) tends to the constant U^* at any fixed time t as $r \uparrow \infty$, the same applies to the total momentum present in the solution.

On the other hand, we note that the type of blowup behavior described by Theorem 6.4 does not depend on the infinite total mass or momentum in the solutions. Indeed, let r = c(t) be any 1-characteristic located outside of the critical 1-characteristic r = $\xi_{\rm w}t$, so that $\mathfrak{c}(0)>0$. We could now replace the given similarity solution in the outer region $\{(r, t) \mid r > c(t)\}$, with a solution (e.g., a simple wave with the same values along r = c(t)) of finite mass in this outer region, without affecting the behavior of the solution in the interior region $\{(r, t) \mid r < c(t)\}$. This shows that the type of amplitude blowup exhibited by the original similarity solution, is possible also in solutions with finite mass.

CRediT authorship contribution statement

Helge Kristian Jenssen: Conceptualization, Formal analysis, Investigation. Charis Tsikkou: Conceptualization, Formal analysis, Investigation.

Acknowledgments

This work was supported in part by the National Science Foundation awards DMS-1813283 (Jenssen) and DMS-1714912 (Tsikkou). The authors would like to thank an anonymous referee whose comments substantially improved the presentation.

Appendix

A.1. Proof of Lemma 3.3

We treat the four inequalities in (3.10) in turn, starting form

the left. We recall that $-m < \beta < 0$, such that $\mu := \frac{\beta}{m} \in (-1,0)$. For the inequality $-\frac{a^2\beta}{a^2m-\lambda_+} < 0$, we observe that, as $\beta < 0$, this is equivalent to $a^2m < \lambda_+$. Substituting from (3.8) for λ_+ , and rearranging, yield the equivalent inequality

$$m - \frac{2}{1+\mu} < \sqrt{(m + \frac{2}{1+\mu})^2 - 8m}.$$
 (A.1)

(Recall from Lemma 3.2 that the radicand is positive for all m and β under consideration.) Since $m \le 2$ and $0 < 1 + \mu < 1$, we have that the left-hand side of (A.1) is negative. As the right-hand side is positive, we conclude that the first inequality of Lemma 3.3 is

The second inequality of Lemma 3.3, i.e., $0 < -\mu$, is immediate

For the inequality $-\mu<-\frac{a^2\beta}{a^2m-\lambda_-}$, substituting $\frac{\beta}{m}$ for μ , and rearranging, yield the equivalent inequality

$$1 < \frac{a^2 m}{a^2 m - \lambda}.\tag{A.2}$$

Recalling from Lemma 3.2 that λ_{-} is positive, we get that (A.2) is satisfied if and only if $\lambda_- < a^2 m$. Substituting from (3.8) for λ_- , and rearranging, yield the equivalent requirement that

$$\frac{2}{1+\mu} - m < \sqrt{(m + \frac{2}{1+\mu})^2 - 8m},\tag{A.3}$$

where the left-hand side is positive due to the argument for (A.1). Squaring both sides in (A.3), and simplifying, give the equivalent requirement that μ < 0, which is satisfied.

Finally, for the fourth inequality of Lemma 3.3, i.e., $-\frac{a^2\beta}{a^2m-\lambda}$ 1, we first use that (as verified above) $a^2m < \lambda_{-}$ to rewrite the inequality as $\lambda_- < a^2(m+\beta)$. Substituting from (3.8) for λ_- , and rearranging, yield the equivalent inequality

$$(\frac{2}{1+\mu}-m)-2\beta<\sqrt{(m+\frac{2}{1+\mu})^2-8m}.$$

The expression in parenthesis on the left-hand side was shown above to be positive; as β < 0, it follows that the left-hand side is a positive number. Thus, by squaring both sides, canceling terms, and simplifying, we obtain that the fourth inequality of Lemma 3.3 is satisfied if and only if

$$\beta^2 - \beta(\frac{2}{1+\mu} - m) < \frac{2m}{1+\mu} - 2m = -\frac{2m\mu}{1+\mu} = -\frac{2\beta}{1+\mu}$$

which reduces further to the inequality $m + \beta > 0$, which is satis field by assumption. This concludes the proof of Lemma 3.3. \Box

A.2. Proof of Lemma 3.4

The claim is that the function

$$L_m(\mu) = \frac{\mu}{1+\mu} + \frac{m(1+\mu)}{(1+2\mu)}\log(2(1+\mu))$$

satisfies $L_m(\mu) < 0$ for $\mu \in (-1, -\frac{1}{2})$, for both m = 1 and m = 2. To see this, we first apply L'Hôpital's rule to obtain that

$$\lim_{\mu\downarrow-1}L_m(\mu)=-\infty,\qquad \lim_{\mu\uparrow-\frac{1}{2}}L_m(\mu)=\frac{m}{2}-1\leq 0.$$

The claim will therefore follow once we establish that $L_m(\mu)$ is strictly increasing on $(-1, -\frac{1}{2})$. We have,

$$\begin{split} L_m'(\mu) &= \frac{1}{(1+\mu)^2} + \frac{m}{(1+2\mu)^2} \left[(1+2\mu) - \log(2(1+\mu)) \right] \\ &> \frac{m}{(1+2\mu)^2} \left[(1+2\mu) - \log(2(1+\mu)) \right]. \end{split}$$

A calculation shows that the function $\mu \mapsto (1+2\mu)-\log(2(1+\mu))$ is strictly positive on $(-1,-\frac{1}{2})$, showing that $L_m'(\mu)>0$ on $(-1,-\frac{1}{2})$. \square

A.3. Proof of Lemma 3.6

Recall that the function \hat{H} is defined by

$$\hat{H}(\xi) := \xi + \frac{a^2}{\hat{U}(\xi) - \xi} \qquad \text{for } 0 < \xi < -\xi_{\mathsf{W}}.$$

We first observe that, by construction, \hat{U} satisfies $\xi - a < \hat{U}(\xi) < \xi$ for $0 < \xi < -\xi_{\rm w}$. Part (i) of Lemma is a direct consequence of this double inequality. For part (ii) we first recall that, according to Lemma 3.1 and the fact that $\hat{U}(\xi)$ is symmetric about the origin in the (ξ, U) -plane, $\hat{U}(\xi)$ approaches 0 with (positive) slope $-\frac{\beta}{n}$ as $\xi \downarrow 0$. Since $-m < \beta < 0$, the slope $-\frac{\beta}{n}$ is less than unity, so that $(\hat{U}(\xi) - \xi) \uparrow 0$ as $\xi \downarrow 0$. It follows that $\hat{H}(\xi)$ tends to $-\infty$ as $\xi \downarrow 0$. Finally, Part (iii) is verified by substituting the values for $\xi_{\rm w}$ and $U_{\rm w}$ given in (3.6). \square

References

- [1] James Glimm, Solutions in the large for nonlinear hyperbolic systems of equations, Comm. Pure Appl. Math. 18 (1965) 697–715, http://dx.doi.org/ 10.1002/cpa.3160180408, MR194770.
- [2] S. Atzeni, J. Meyer-ter Vehn, The Physics of Inertial Fusion, in: International Series of Monographs on Physics, vol. 125, Oxford University Press, Oxford, 2004.
- [3] R. Courant, K.O. Friedrichs, Supersonic Flow and Shock Waves, Springer-Verlag, 1976, p. xvi+464, Reprinting of the 1948 original; Applied Mathematical Sciences, Vol. 21, MR0421279 (54 #9284).
- [4] G. Guderley, Starke kugelige und zylindrische Verdichtungsstösse in der Nähe des Kugelmittelpunktes bzw. der Zylinderachse, Luftfahrtforschung 19 (1942) 302–311, MR0008522.
- [5] L.I. Sedov, Similarity and Dimensional Methods in Mechanics, "Mir", Moscow, 1982, p. 424, Translated from the Russian by V. I. Kisin. MR603457

- [6] K.P. Stanyukovich, Unsteady Motion of Continuous Media, Pergamon Press, New York-London-Oxford-Paris, 1960, p. xiii+745, Translation edited by Maurice Holt; literal translation by J. George Adashko. MR0114423.
- [7] C. Hunter, On the collapse of an empty cavity in water, J. Fluid Mech. 8 (1960) 241–263.
- [8] Roger B. Lazarus, Self-similar solutions for converging shocks and collapsing cavities, SIAM J. Numer. Anal. 18 (2) (1981) 316–371.
- [9] Scott D. Ramsey, James R. Kamm, John H. Bolstad, The guderley problem revisited, Int. J. Comput. Fluid Dyn. 26 (2) (2012) 79–99, http://dx.doi.org/ 10.1080/10618562.2011.647768, MR2892836.
- [10] Helge Kristian Jenssen, Charis Tsikkou, On similarity flows for the compressible Euler system, J. Math. Phys. 59 (12) (2018) 121507, 25, http://dx.doi.org/10.1063/1.5049093, MR3894017.
- [11] Constantine M. Dafermos, Hyperbolic Conservation Laws in Continuum Physics, fourth ed., in: Grundlehren der Mathematischen Wissenschaften [Fundamental Principles of Mathematical Sciences], vol. 325, Springer-Verlag, Berlin, 2016, xxxviii+826. MR3468916. http://dx.doi.org/10.1007/ 978-3-662-49451-6.
- [12] Gui-Qiang G. Chen, Mikhail Perepelitsa, Vanishing viscosity solutions of the compressible Euler equations with spherical symmetry and large initial data, Comm. Math. Phys. 338 (2) (2015) 771-800, MR3351058.
- [13] Gui-Qiang G. Chen, Matthew R.I. Schrecker, Vanishing viscosity approach to the compressible Euler equations for transonic nozzle and spherically symmetric flows, Arch. Ration. Mech. Anal. 229 (3) (2018) 1239–1279, http://dx.doi.org/10.1007/s00205-018-1239-z. MR3814602.
- [14] Matthew R.I. Schrecker, Spherically symmetric solutions of the multidimensional, compressible, isentropic Euler equations, 2019, arXiv:1901. 00736
- [15] Matthew R.I. Schrecker, Private communication.
- [16] Gui-Qiang Chen, Tian-Hong Li, Global entropy solutions in L^{∞} to the Euler equations and Euler-Poisson equations for isothermal fluids with spherical symmetry, Methods Appl. Anal. 10 (2) (2003) 215–243, MR2074749.
- [17] Tetu Makino, Kiyoshi Mizohata, Seiji Ukai, The global weak solutions of compressible Euler equation with spherical symmetry, Japan J. Indust. Appl. Math. 9 (3) (1992) 431–449, http://dx.doi.org/10.1007/BF03167276, MR1189949.
- [18] Tetu Makino, Kiyoshi Mizohata, Seiji Ukai, Global weak solutions of the compressible Euler equation with spherical symmetry. II, Japan J. Indust. Appl. Math. 11 (3) (1994) 417–426, http://dx.doi.org/10.1007/BF03167230, MR1299954.
- [19] Yuxi Zheng, Systems of Conservation Laws, in: Progress in Nonlinear Differential Equations and their Applications, vol. 38, Birkhäuser Boston Inc., 2001, p. xvi+317, Two-dimensional Riemann problems. MR1839813 (2002e:35155).
- [20] David Hoff, Spherically symmetric solutions of the Navier–Stokes equations for compressible, isothermal flow with large, discontinuous initial data, Indiana Univ. Math. J. 41 (1992) 1225–1302.
- [21] J.B. Keller, Spherical, cylindrical and one-dimensional gas flows, Quart. Appl. Math. 14 (1956) 171–184.